Advanced Modeling and Control Strategies for Charging Electric Vehicle Batteries

A THESIS

SUBMITTED TO THE FACULTY OF

THE UNIVERSITY OF MINNESOTA

BY

Murtaza Kamal Pasha Khan

IN PARTIAL FULFILLMENT OF THE REQUIREMENTS

FOR THE DEGREE OF

MASTER OF SCIENCE

October, 2019

Acknowledgement

This work was supported by the Energy, Power, Control and Network (EPCN) program of the National Science Foundation under a Grant Number of 171167. This innovative research project on control and optimization gives me a wonderful opportunity to work as a Research Assistant under the supervision of Dr. Desineni Subbaram Naidu. Over the course of 2 years at the University of Minnesota Duluth (UMD), I had wonderful time with him and I found him inspiring, jovial,thoughtful and pro-active. I'm expressing my utmost gratitude to him for giving me a chance to work in this project.

Secondly, I'm expressing my appreciation and gratitude to Dr. Mohammed Hasan and Dr. PS Dhanasekaran for serving as committee members of this thesis. Their sincere advice and corrections have made this work more presentable.

I would like to thank the Electrical Engineering Department of UMD for allowing me to pursue my MSEE. As a graduate student, I had the great pleasure of serving as a TA in several different courses. I am grateful for funding that was available for me. The experience I gathered from here was super and has laid a solid foundation for me to advance my career as a professor.

Lastly, I want to thank my mother, family members and friends for their continuous support.

Contents

List of Figures

Abstract

The research in this master's thesis presents an advanced modeling and control strategy for charging electric vehicle (EV) batteries. The purpose of modeling the battery incorporating the optimal control mechanism is developing a fast-charging system for EVs. The thesis starts with a literature survey to find out the latest EV battery model within an appropriate format of interest. Then, on the selected battery model, it applies the state-dependent Riccati equation (SDRE) technique to develop a closed-loop optimal control strategy. For the purpose of optimization, the battery model aims to track a reference trajectory with a performance index which is minimizing the quadratic error between a reference and an actual trajectory. To harness the unified benefits of optimal and intelligent control systems, the thesis also sheds light upon fuzzy logic by generating a reference trajectory with it. Finally, to determine the correctness of the modeling, MATLAB simulations for a lithium-ion (li-ion) battery have been carried out and they display a satisfactory tracking performance.

Chapter 1

Introduction

Challenges and opportunities of integrating electric vehicles (EV) with an electric grid have been of great interest for the past few years. In order to integrate with an electric grid, a battery model of the EV should have adequate control mechanisms. In this thesis, optimal control of a battery is a prime focus. For developing the control mechanism, a closed-loop optimal control strategy is obtained by using the State-Dependent Riccati Equation (SDRE) technique with performance index to minimize the quadratic error between the reference and actual trajectories. Before that, an extensive literature survey was conducted to find a suitable battery model for EV applications.

1.1 Literature Survey for a Battery Model

Battery modeling means knowing the ins and outs of a battery, for example, knowing current, voltage, parameters of that battery. In addition, thousands of models were considered by different researchers for different purposes. A model can work

for a suitable purpose, but may not work for a different purpose. At the beginning of this research, many contemporary models were studied to figure out the best model for the purpose of this research. First, researchers presents a battery with an equivalent circuit model that consists of a single voltage source, single series resistor and a single RC block to express a simulation model of lithium cells [13]. They used MATLAB design optimization toolbox for performing an estimation of parameters for the model. Results of the estimation show that the circuit parameters depend on the state of charge (SOC), average current and temperature. It should be noted that the parameter estimation app uses a pulse current discharge test on high power lithium cells. One of the researchers from this research along with other researchers continued their research and developed a battery model that overcame few weaknesses of its predecessor [14]. In this updated battery model which aims to estimate accurate run-time SOC of a lithium iron phosphate (LFP) cell, cells are renowned for high intrinsic safety, fast charging and long cycle life. The developed model was a novel combination of the extended Kalman filtering (EKF) algorithm, two-RC-block equivalent circuit and traditional coulomb counting method. This novel combination solved three key shortcomings of the traditional SOC estimation method (coulomb counting method) and resulted in an efficient estimation method. Next,in [30], a new electric vehicle battery charging/discharging strategy was discussed in detail. This new technology consists of bidirectional DC/DC converter. The simulation model of the charging/discharging was validated using control techniques. The charging and discharging technique of an EV battery was further elaborated in [2]. A CHAdeMO (trade name of a quick charging method for battery electric vehicles) protocol based fast charging technology for EVs was proposed. This simulation-based proposal has two main parts, which will communicate with each other by CAN bus. The two main parts are (1) the electric vehicle and its battery management system and (2) a charging/discharging device emulated by a computer application. The model also

proposed a data model for both electric vehicle and charging/discharging device to manage the charging/discharging process according to a power network operator. An unique method for parameter estimation was proposed in [1]. Electric vehicles gain wide recognition for their supremacy over fossil-fuel powered vehicles as a more efficient and sustainable transportation alternative. Battery wear is an important topic because the model of the battery changes as it ages. To effectively capture this characteristic, Ahmed, Gazzarri, Onori, Habibi, Jackey, Rzemien, Tjong & LeSage presented an effective method for offline battery model parameter estimation at various states of health. Three lithium nickel-manganese-cobalt oxide ($LiNiMnCoO_2$) cells were at temperatures ranging from 35°C to 40°C. The model resulted in look-up tables for equivalent circuit parameters. The results also indicated aging effects demand remodeling of the equivalent circuit as in the beginning of battery life. The model shows 5 R-C pairs can precisely describe cell dynamics of a battery cell. Further in [33], Wijewardana, Vepa and Shaheed presented a suitable, convenient and generic representation of battery dynamics to model any li-ion rechargeable battery. With application to state of charge (SOC) estimation, this model included thermal balance of heat generation mechanism, ambient temperature effect, storage effects, cyclic charging, battery internal resistance and SOC to model a li-ion battery. Next, a thermo-dependent advanced hybrid li-ion battery model, consisting of empirical and artificial neural network submodels were developed for a system level analysis of electric vehicle fleet simulation and distributed energy storage application. Simulation showed this model successfully determined battery voltage and estimated SOC [20]. In another research, Ramadan, Claude & Becherif have designed and validated a battery management systems (BMS) for li-ion batteries. The integration of BMS ensures the sustainable battery operation of hybrid electric vehicles (HEVs) by correctly measuring battery SOC, state of health (SOH) and instantaneous power. To design BMS, they developed electri-

cal battery model and mathematical equations. Then parameters of the battery were identified using voltage drop measurements. Finally, with the application of extended kalman filtering (EKF), the SOC of the model was determined [7]. An important charging/discharging method was presented by a mathematical model with positive and negative materials of $LiyMn_2O_4$ and $LixC_6$ for simulating the electrochemical behaviors of li-ion batteries. Open circuit voltage, current, SOC and charging/discharging characteristics of the battery were considered to present the model. Simulation results showed that the model demonstrates accurate battery charging/discharging strategies and SOC measurement techniques [11]. Finally, a parameter based battery is modeled in [4]. This model is actually a modified curve-fitting version of [19]. Here, parameters V_{OC}, R_{series}, R_{sec}, C_{sec}, R_{min}, C_{min}, R_{hour}, C_{hour} depend on SOC and temperature. A polynomial equation shown in (equation 1.1.1) represent the parameters. Values of all these parameters can be extracted if the constants a_0 through a_6 are known. In this paper [4] Experimental values of these constants are given in a tabular form. Therefore, using values from the table, parameters can be retrieved properly.

$$\mathbf{ln(V, R, C) = (a_0) + (a_1)ln(SOC) + ... + (a_6)ln^6(SOC)} \tag{1.1.1}$$

Figure 1.1 shows the model of this circuit. Parameters of this circuit is calculated

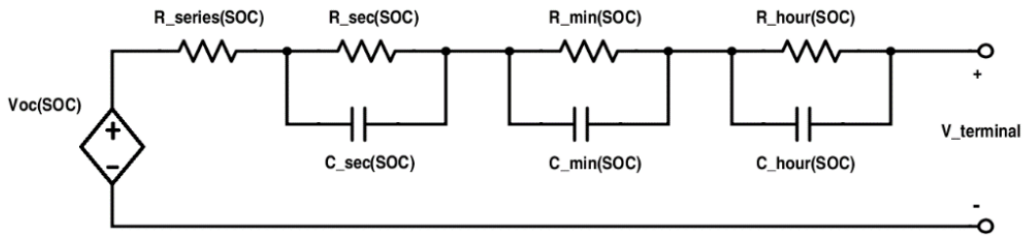

Figure 1.1: 3-RC Branched Battery Model

in different time-scales, for example in minutes, seconds and hours. The objective of doing this is measuring short and long term transients precisely.

1.2 Statement of the Problem

EV battery models are nonlinear and require controlling techniques that are able to analyze nonlinear systems. Optimal charging is such a technique which maximizes the total power that can be delivered to the vehicles while operating within network limits. Therefore, the scope of this work involves optimal control (also known as hard control) and soft control (SC) for battery charging for plug-in electric vehicles. This includes new charging strategy for the battery modelled from principles of physics and model predictive methods.

1.3 Objective of the Thesis

Development of a nonlinear, finite horizon, closed loop optimal tracking controller using state dependent Riccati Equation (SDRE). In designing the optimal controller, state of charge (SOC) will be considered as a state variable. And the optimal controller will be developed first only with hard control (HC) techniques and second with a fusion of HC and SC techniques. The performance of the controller will be judged by its tracking ability of a given trajectory or a reference voltage. In brief, the output or terminal voltage of an EV battery should follow a given trajectory (charging profile).

1.4 Overview of the Thesis

This dissertation is composed of **five** chapters covering the following topics:

1. Chapter 2 provides a detail discussion on battery modeling. In particular, discussions on a generic li-ion battery model, 3-RC battery model and a dual RC battery model is provided in this chapter. In addition, MATLAB simulation for the generic li-ion model also provided.

2. Chapter 3 starts with a discussion on optimal control and state dependent Riccati equation (SDRE) technique. Then, it shows the whole procedure of treating a finite-horizon tracking problem with SDRE technique. Finally, a discussion on soft control techniques concludes the chapter.

3. Chapter 4 explains the applicability of the simulation results obtained from MATLAB simulations. At the end of the chapter, it describes ways to improve the results.

4. Finally, Chapter 5 presents the conclusion of the work with a note on future improvement scopes.

The summary of the thesis work was also submitted as a manuscript titled, "Advanced Tracking Strategies for Charging Electric Vehicle Batteries", authored by Murtaza Kamal Pasha Khan, Dr. Desineni Subbaram Naidu and Dr. Ona Egbue for the eleventh Conference on Innovative Smart Grid Technologies (ISGT 2020), sponsored by the IEEE Power & Energy Society (PES), will be held on February 17-20, 2020 at the Grand Hyatt Washington, Washington DC. This submitted manuscript is also attached with this thesis in appendix 2.

Chapter 2

Battery Modeling

2.1 Simple Battery Model

A generic battery model for a dynamic simulation of hybrid electric vehicle is discussed in [31], the nonlinear battery model is shown in Figure 2.1. This model consists of a controlled voltage source and an internal resistance. Simulation results of this easy-to use model is shown in Figure 2.2. This figure illustrates the performance of a 7.2 volts, 5.4 Ampere-hour li-ion battery model. In the figure, voltage vs time, current vs time and SOC vs time response of the generic battery is plotted. Here, temperature effect on battery parameter is neglected and only SOC is considered as a state variable. The model is plotted in MATLAB with the help of Simscape Power System toolbox. In figure 2.1, an equation for controlled voltage source is given. Here, E = no-load voltage (V), E_0 = battery constant voltage (V), K = polarisation voltage (V), Q = battery capacity (Ah),$\int idt$ = actual battery charge (Ah), A= exponential zone amplitude (V), B= exponential zone time constant inverse $(Ah)^{-1}$, V_{batt}= battery voltage (V), R=internal resistance (ohms), and

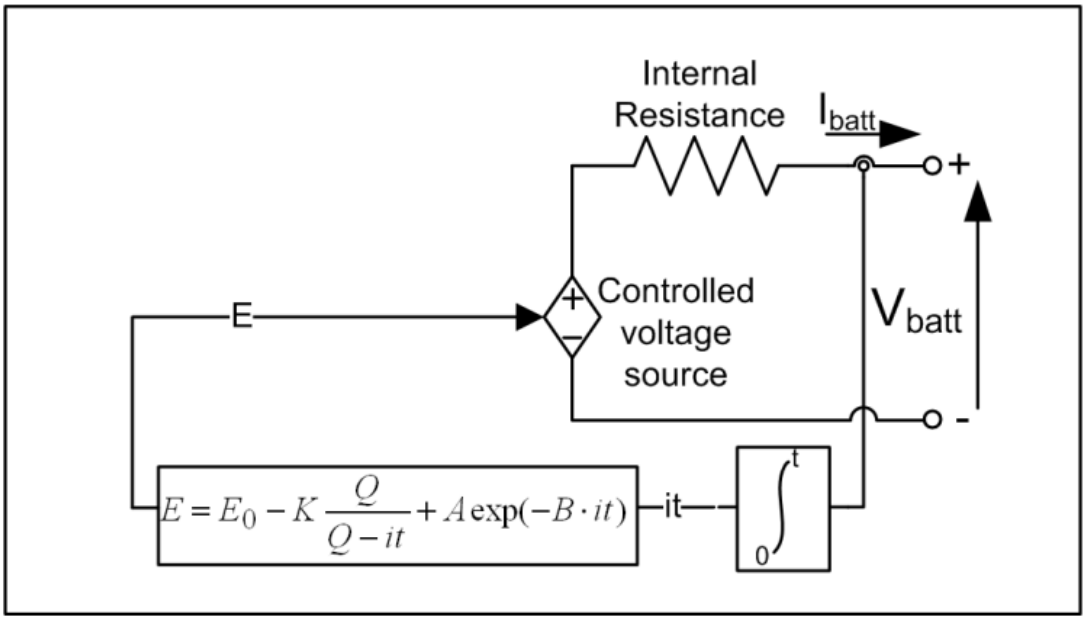

Figure 2.1: Nonlinear Battery Model

i=battery current (A).

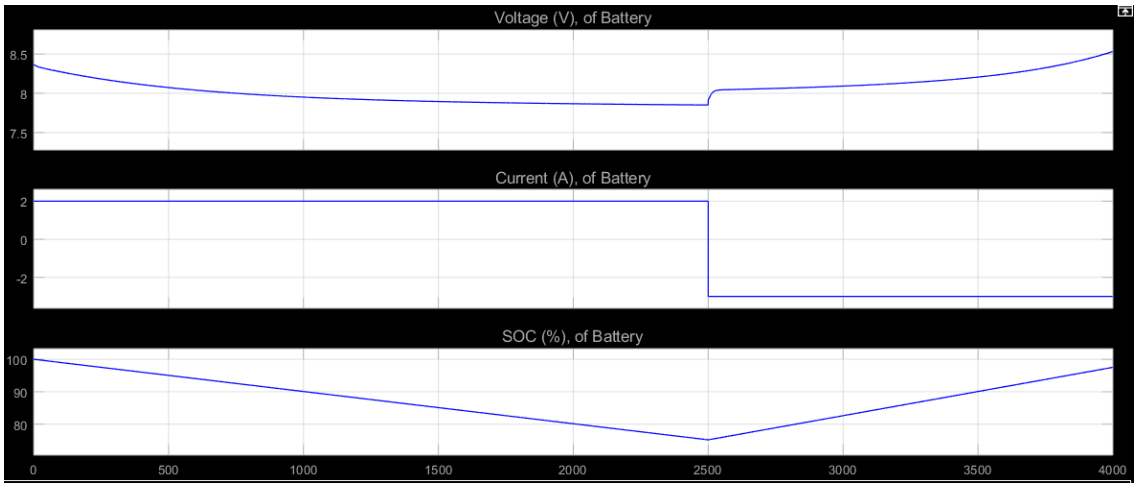

Figure 2.2: Current, Voltage and SOC of a li-ion Battery

2.2 Three RC Model

A comparative study on a number of battery models was provided in [22]. A Detailed explanation was given on models such as Shepherd model, Randles model and Thevenin model. Shepherd model is the simplest in terms of the parameter estimation, however, it has a relative error of more than 10 units when a driving cycle was applied. The Randles model, even though is good for applications with voltage variations lower than 5 volts, did not reflect the actual dynamics of a battery. On the other hand, Thevenin electrical equivalent circuit model (EECM) showed robustness under fast variations of current and voltage. Second, It has only a relative error of below 5% when ECE15 drive cycle was applied. In addition, it is best in reproducing the chemical behaviors of an EV battery. Therefore, thevenin equivalent circuit is most suitable for EV applications. The model of the circuit is shown in Figure 2.3.

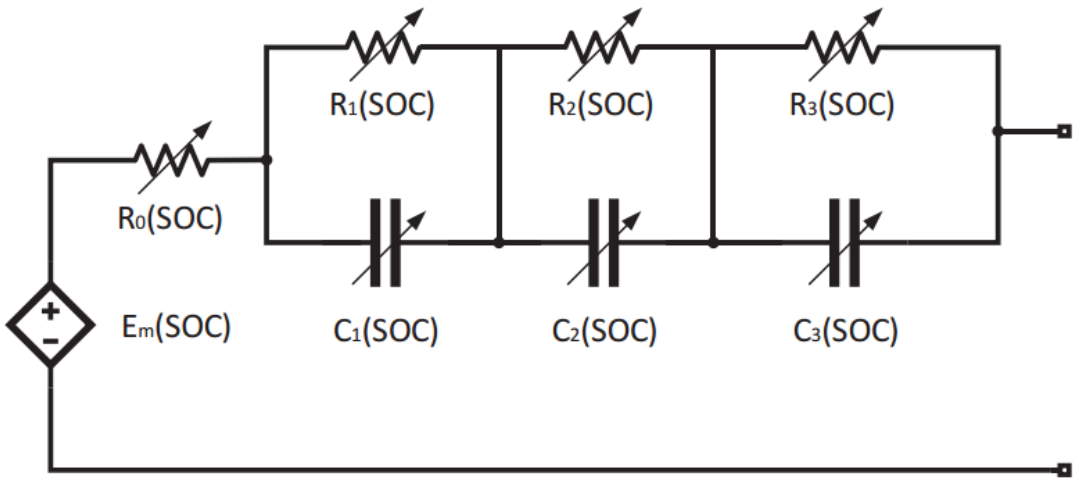

Figure 2.3: Electric Thevenin Model with 3 RC-Branches

Here, the model includes an internal resistance $R_0(SOC)$ parameter, which is a SOC dependent element. In fact, all the parameters of this model is dependent on SOC. Elements such as E_m represents open circuit voltage and R_1,R_2, R_3, C_1,C_2,

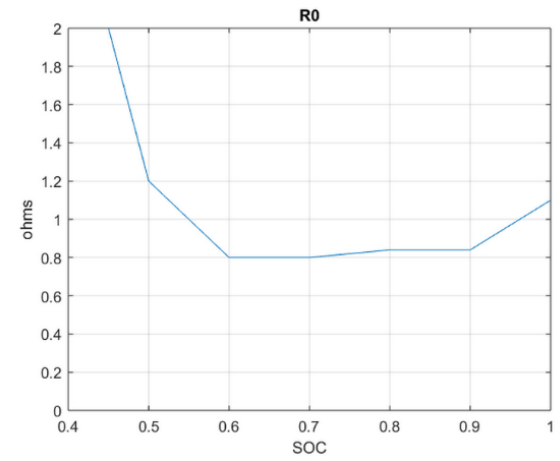

(a) R0

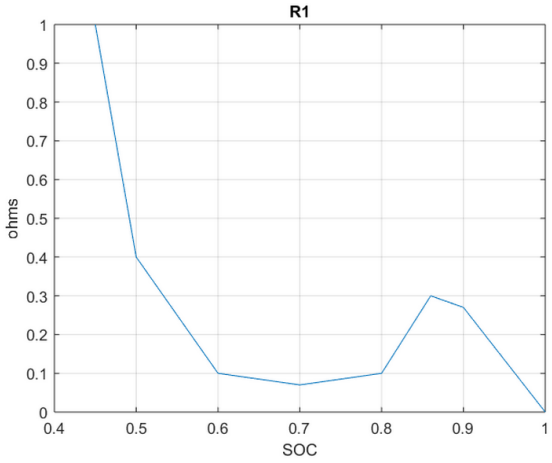

(b) R1

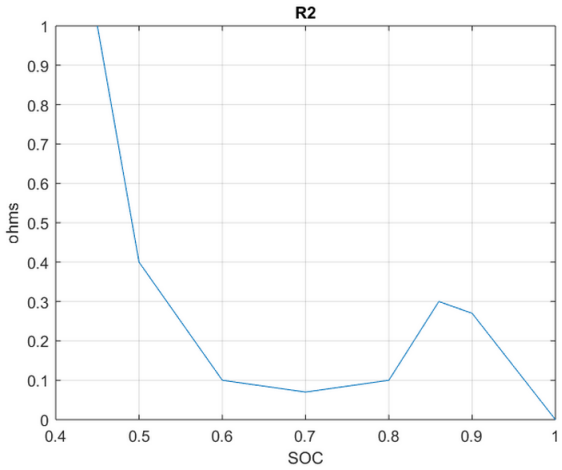

(c) R2

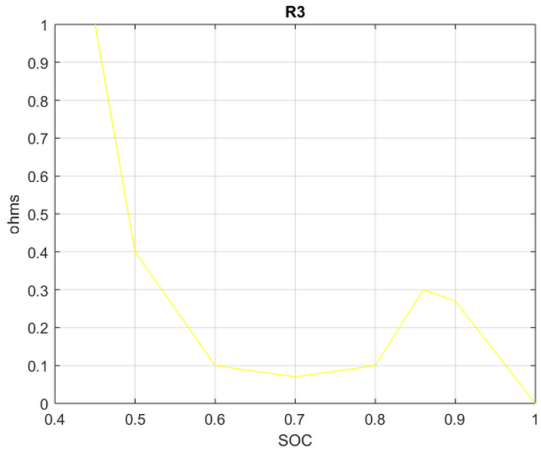

(d) R3

Figure 2.4: Parameter Estimations

C_3 represent the elements of a bias network. The parameter estimation for this 3-branched model is complicated and requires more look up tables. Figure 2.4 and Figure 2.5 show the estimated parameter values. Parameters were estimated from a MATLAB parameter estimation toolbox. These pictorial presentation describes the parameter values with respect to the full range of SOC *(0 to 1)*. Therefore, SOC vs voltage or capacitance or resistance are measured for the respective cases.

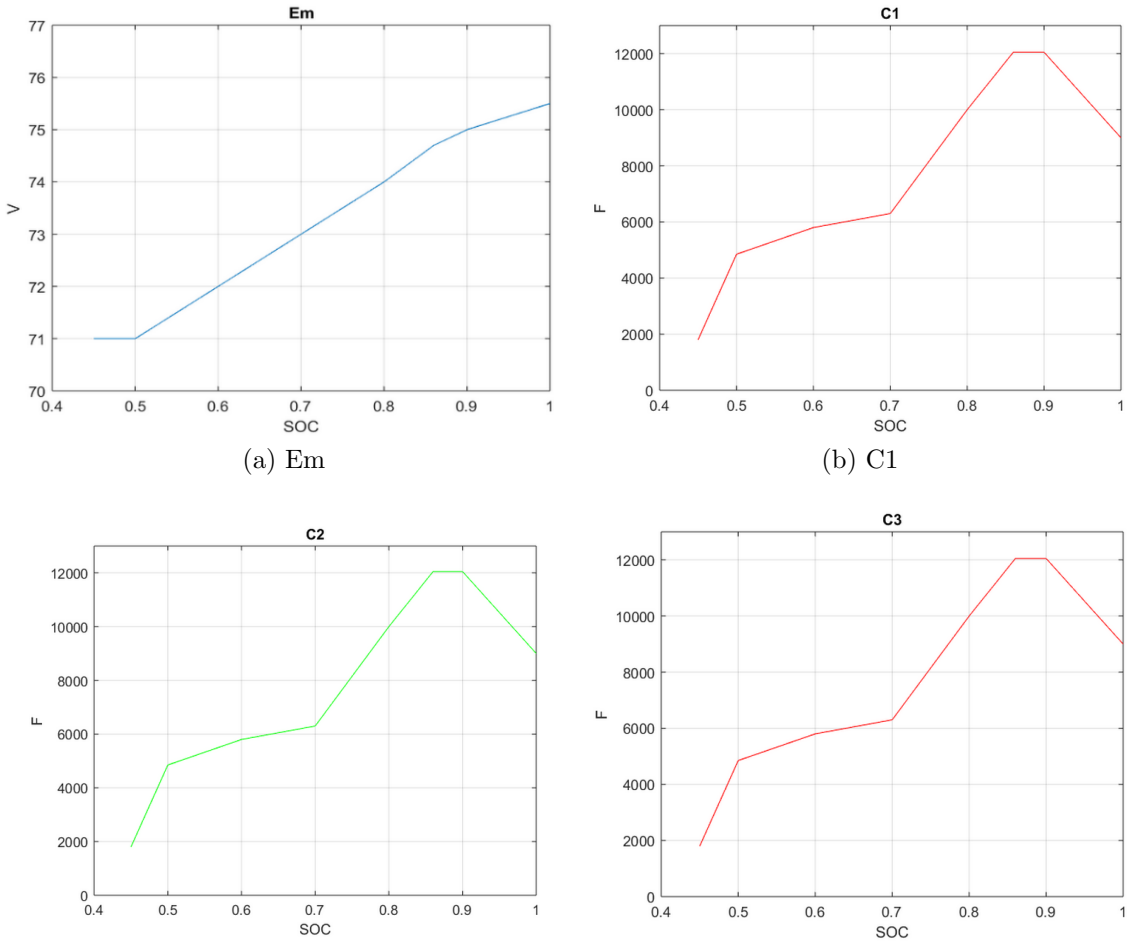

(a) Em (b) C1

(c) C2 (d) C3

Figure 2.5: Parameter Estimations(contd.)

2.3 Dual RC Model

A second-order RC (2 RC) (shown in Figure 2.6) EECM with nonlinear dynamic equations is used to investigate the output or terminal characteristics of a lithium-ion (li-ion) battery under different charging/discharging and temperature conditions. This dual RC model is considered for its good balance between complexity and accuracy. The circuit model consists of R_0, R_1, C_1, R_2 and C_2, where R_0 indicates the instantaneous voltage drop of the battery terminal voltage, and the RC

networks expresses the long-term and short-term transient behavior of the battery and all the elements are SOC dependent.For this model, the states are two capacitor voltages and SOC. The capacitor voltages are kept equal because they are equal at the beginning of the simulation[12]. Dynamic equations of the circuit elements are given below [9],[25],[29],[28].

$$\begin{aligned} V_{OC}(SOC) = &- 1.031.exp^{-35*SOC} + 3.685 + 0.2156 * SOC \\ &- 0.1178 * SOC^2 + 0.3201 * SOC^3 \end{aligned} \tag{2.3.1}$$

$$R_0(SOC) = -0.1562.exp^{-24.37*SOC} + 0.07446 \tag{2.3.2}$$

$$R_1(SOC) = -0.3208.exp^{-29.14*SOC} + 0.04669 \tag{2.3.3}$$

$$C_1(SOC) = -752.9exp^{-13.51*SOC} + 703.6 \tag{2.3.4}$$

$$R_2(SOC) = -6.603.exp^{-155.2*SOC} + 0.04984 \tag{2.3.5}$$

$$C_2(SOC) = -6056.exp^{-27.12*SOC} + 4475 \tag{2.3.6}$$

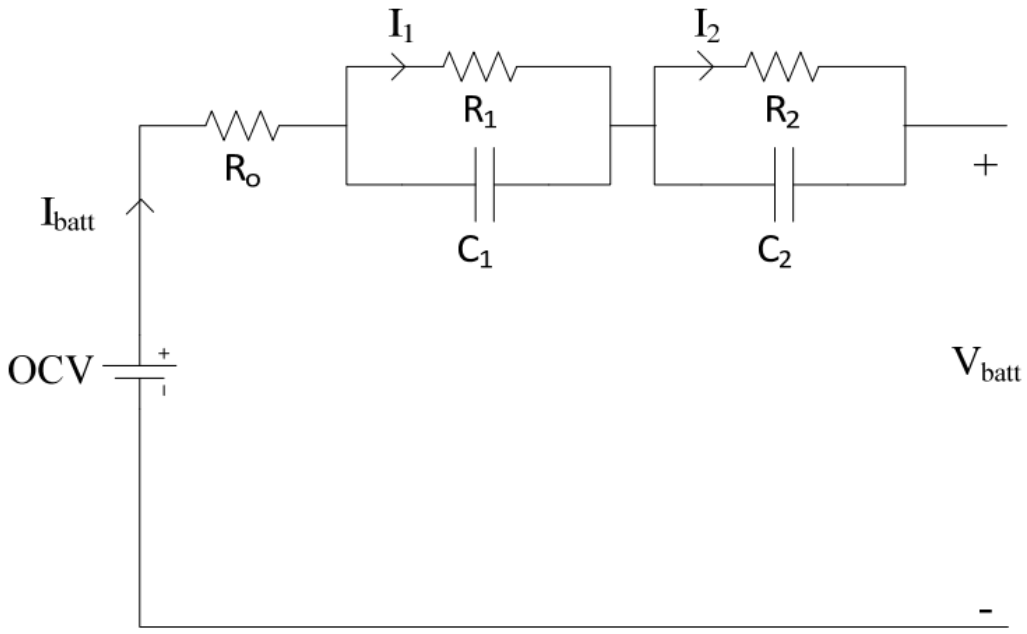

Figure 2.6: 2-RC Branched Battery Model

2.3.1 Battery State-Space Model

The dynamics of this dual RC model can also be expressed in state-space form, which is also a desired state dependent coefficient (SDC) form for this battery model. An appropriate SDC form of a nonlinear model makes it controllable or at least stable. Hence, expressing it in a SDC form is very crucial for optimal control applications.

$$\dot{x}(t) = Ax(t) + Bu(t) \tag{2.3.7}$$

Matrices A and B are SOC dependent. So, $A(SOC)$ is $n - by - n$ state matrix, $B(SOC)$ is $n - by - r$ control matrix and the control signal $u(t)$ is unconstrained. Equation 2.3.1 is also a desired SDC form of this system. And the parameters

$A(SOC)$ and $B(SOC)$ are

$$\mathbf{A(SOC)} = \begin{bmatrix} A_{11} & 0 & 0 \\ 0 & A_{22} & 0 \\ 0 & 0 & 0 \end{bmatrix}$$

and,

$$\mathbf{B(SOC)} = \begin{bmatrix} B_{11} \\ B_{21} \\ B_{31} \end{bmatrix}$$

where,

$$A_{11} = \frac{-1}{R_1(SOC)C_1(SOC)},$$
$$A_{22} = \frac{-1}{R_2(SOC)C_2(SOC)},$$
$$B_{11} = \frac{1}{C_1(SOC)},$$
$$B_{21} = \frac{1}{C_2(SOC)},$$
$$and$$
$$B_{31} = \frac{-\eta}{Q},$$

Here, η represents coulombic efficiency (energy loss) of the battery. It is assumed 1 for this study . Q, a constant, expresses total capacity or maximum coulomb hours of a battery. The input $u(t)$ of this circuit is $I(t)$, it is a constant current profile and it is assumed $1A$ for this study. The output equation of the battery/terminal

voltage equation of the battery can be expressed as

$$y(t) = V_{batt} = V_{OC}(SOC) - V_1(SOC) - V_2(SOC) - R_0(SOC).I(t), \tag{2.3.8}$$

V_1 and V_2 is calculated by applying Kirchhoff's law,

$$\dot{V_1}(SOC) = \frac{-V_1(SOC)}{R_1(SOC)C_1(SOC)} + \frac{u(t)}{C_1(SOC)}, \tag{2.3.9}$$

$$\dot{V_2}(SOC) = \frac{-V_2(SOC)}{R_2(SOC)C_2(SOC)} + \frac{u(t)}{C_2(SOC)} \tag{2.3.10}$$

So, the state space representation of the battery model is

$$\begin{bmatrix} \dot{x_1} \\ \dot{x_2} \\ \dot{x} \end{bmatrix} = \begin{bmatrix} A_{11} & 0 & 0 \\ 0 & A_{22} & 0 \\ 0 & 0 & 0 \end{bmatrix} \begin{bmatrix} x_1 \\ x_2 \\ x \end{bmatrix} + \begin{bmatrix} B_{11} \\ B_{21} \\ B_{31} \end{bmatrix} \begin{bmatrix} u \end{bmatrix} \tag{2.3.11}$$

Here, x_1 and x_2 is the voltage drop across the capacitor and x is the state of charge (SOC). These three are state variables of the system. Note that, SOC is not estimated in this work rather it is taken as a state. Therefore, when SDRE is in effect, SOC changes in each iteration.

Chapter 3

Hard and Soft Control Techniques

3.1 Optimal Control

Optimal control aims to optimize a plant (process) by finding a control input. To obtain a control input, optimal control minimize or maximize a process by satisfying a specific performance criterion. The plant should have following three characteristics in order to be considered as an optimal control problem:

1. A mathematical model of the plant that need to be controlled. The model generally expressed as a dynamic system with state variables.

2. Description of a performance index such as reaching a target in a minimal amount of time.

3. Description of boundary conditions or physical constraints needed to exceed to reach the target.

An optimal control problem generally derived by Pontryagin's minimum principal or by Hamilton-Jacobi-Bellman (HJB) equation. In addition, calculus of variation

plays significant role to obtain a solution for optimal control problems. Examples of optimal control problems are

1. Reaching moon with minimum fuel expenditure (Fuel- Optimal Control System). Mathematical model for this system would be a dynamic system of a spacecraft with associated state variables such velocity, thrust of a rocket.

2. Reaching from point A to point B in minimal time, etc.

3. Some of the areas that can be optimally controlled are biomedical systems, aerospace systems, automotive systems etc.

A vast majority of these systems are nonlinear and they contain differential terms. Therefore, an urgent need for nonlinear control systems has increased over the last decades, which has led to develop nonlinear control system techniques. On such technique is state dependent Riccati equation (SDRE), which is explained in the following section.

3.1.1 Fundamentals of SDRE

Emerged from the celebrated algebraic Riccati equation (ARE) [5, 8], SDRE also referred to as the Frozen Riccati Equation (FRE) which is able to approximate the solution of a nonlinear system at each instant of time. First, the algorithm transforms a non-linear system into a linear like structure and minimizes a non-quadratic performance index to a quadratic-like structure. Then it approximates a solution that depends on solving the algebraic Riccati equation (ARE) for the steady state value and applies a change of variables procedure [27] to convert a differential Riccati equation (DRE) to a linear differential Lyapunov equation (DLE) [26]. Finally, the procedure evaluates the coefficients of the resulting equations based on the current state values at each time interval and freezes these coefficients from current

time to the next time step. The Lyapunov equation is solved in a closed form at each interval during online implementation. The use of Lyapunov-type equations in solving optimal problems is given in [32].

3.1.2 Applications of SDRE

In the last decade, SDRE become widely renowned among the control community for its effectiveness in designing nonlinear feedback controller. Applications of SDRE method can be found in various areas such as tracking a robotic arm. Arm motions, made of kinetic energy and potential energy equations are nonlinear. With the help of these nonlinear equations, a nonlinear dynamic system was constructed and optimal tracking theory was applied. Simulations show a successful result as a Two-link finger (thumb) and a three-link finger (index) track a sinusoidal trajectory[15].Next, in a different research, a combination of the state-dependent differential Riccati equation technique and Kalman filtering algorithm gives satisfactory results in designing a controller for wind energy conversion system (WECS). Kalman filtering algorithm was used to measure corrupted nonlinear states of the system[17]. In recent past, in a different work, researchers proposed a simplified approach for SDRE technique. This approach doesn't assume SDRE coefficients constant during the small intervals of the finite horizon period and finds sub-optimal solution. The novel theory is validated by designing a control for sixth order variable speed, variable pitch wind energy conversion system[24].

3.2 Finite-Horizon Nonlinear Systems

In this section, the control technique that was applied on the EV battery model is explained. We are considering a finite horizon non-linear deterministic system.

The section shows step-by-step, how a nonlinear system can be formed and how to obtain a solution for the above case.

3.2.1 Statement of the Problem

Suppose, the nonlinear system is,

$$\dot{\mathbf{x}}(t) = \mathbf{f}(\mathbf{x}) + \mathbf{g}(\mathbf{x})\mathbf{u}(t), \tag{3.2.1}$$

$$\mathbf{y}(t) = \mathbf{h}(\mathbf{x}), \tag{3.2.2}$$

where, $\mathbf{x}$ is *nth* state vector, $\mathbf{u(t)}$ is *rth* control vector and $\mathbf{y(t)}$ is *mth* output vector. The system is transformed to a linear-like structure, which termed as state dependent coefficient (SDC) form,

$$\dot{\mathbf{x}}(t) = \mathbf{A}(\mathbf{x})\mathbf{x}(t) + \mathbf{B}(\mathbf{x})\mathbf{u}(t), \tag{3.2.3}$$

$$\mathbf{y}(t) = \mathbf{C}(\mathbf{x})\mathbf{x}(t), \tag{3.2.4}$$

where, $\mathbf{f}(\mathbf{x}) = \mathbf{A}(\mathbf{x})\mathbf{x}(t)$, $\mathbf{B}(\mathbf{x})= \mathbf{g}(\mathbf{x})$, and $\mathbf{h}(\mathbf{x}) = \mathbf{C}(\mathbf{x})\mathbf{x}(t)$. Here, $\mathbf{A(x)}$ is *n-by-n* state matrix and $\mathbf{B(x)}$ is *n-by-r* control matrix. The goal is to obtain a state feedback optimal control of the form $\mathbf{u}(\mathbf{x},t) = -\mathbf{K}(\mathbf{x},t)\mathbf{x}(t)$, which minimizes a cost function [23] given as,

$$\begin{aligned}\mathbf{J}(\mathbf{x},\mathbf{u}) = &\frac{1}{2}\mathbf{x}'(t_f)\mathbf{F}\mathbf{x}(t_f)+ \\ &\frac{1}{2}\int_{t_0}^{t_f}\left[\mathbf{x}'(t)\mathbf{Q}(\mathbf{x})\mathbf{x}(t) + \mathbf{u}'(\mathbf{x})\mathbf{R}(\mathbf{x})\mathbf{u}(\mathbf{x})\right]\,dt,\end{aligned} \tag{3.2.5}$$

where, $\mathbf{Q}(\mathbf{x})$ is *n-by-n* dimensional error weighted matrix and $\mathbf{R}(\mathbf{x})$ is *r-by-r*

dimensional control weighted matrix. In order to keep the closed loop error $\mathbf{e(t)}$ small and error squared non-negative, $\mathbf{Q(x)}$ must be a *positive semi-definite* matrix. For the same purpose, the other requirements should be fulfilled, such as terminal cost weighted matrix $\mathbf{F}$ (also *n-by-n* dimensional) should be symmetric and *positive semi-definite* and the control weighted matrix, $\mathbf{R(x)}$ must be a symmetric *positive definite* matrix. $\mathbf{x}'(t)\mathbf{Q(x)x}(t)$ is a measure of state accuracy and $\mathbf{u}'(\mathbf{x})\mathbf{R(x)u(x)}$ is a measure of control effort.

3.2.2 Finite-Horizon Tracking for Deterministic Nonlinear Systems

Consider the given nonlinear state-dependent system (3.2.3) and (3.2.4) and $\mathbf{z}(t)$ is the *desired* output or trajectory. The goal is to eliminate the closed-loop error by minimizing the given cost function

$$\mathbf{J(x,u)} = \frac{1}{2}\mathbf{x}'(t_f)\mathbf{Fx}(t_f) + \frac{1}{2}\int_{t_0}^{t_f} \left[\mathbf{x}'(t)\mathbf{Q(x)e}(t) + \mathbf{u}'(\mathbf{x})\mathbf{R(x)u(x)}\right]\, dt, \qquad (3.2.6)$$

where the closed-loop error $\mathbf{e}(t) = \mathbf{z}(t) - \mathbf{y}(t)$.

3.2.3 Solution for Finite-Horizon Tracking Problem

The optimal closed-loop control input is given as

$$\mathbf{u(x)} = -\mathbf{R}^{-1}\mathbf{B}'(\mathbf{x})[\mathbf{P(x)x} - \mathbf{g(x)}] \qquad (3.2.7)$$

where $\mathbf{P(x)}$, is symmetric and positive-definite, and is the solution of the differ-

ential Riccati equation (SDRE) that is given by

$$-\dot{\mathbf{P}}(\mathbf{x}) = \mathbf{P}(\mathbf{x})\mathbf{A}(\mathbf{x}) + \mathbf{A}'(\mathbf{x})\mathbf{P}(\mathbf{x}) - \mathbf{P}(\mathbf{x})\mathbf{B}(\mathbf{x})\mathbf{R}^{-1}\mathbf{B}'(\mathbf{x})\mathbf{P}(\mathbf{x}) + \mathbf{C}'(\mathbf{x})\mathbf{Q}(\mathbf{x})\mathbf{C}(\mathbf{x}) \tag{3.2.8}$$

with the final condition

$$\mathbf{P}(\mathbf{x}, t_f) = \mathbf{C}'(t_f)\mathbf{F}\mathbf{C}(t_f) \tag{3.2.9}$$

and $\mathbf{g}(\mathbf{x})$ is a solution of the state-dependent non-homogeneous VDE which has the form

$$\dot{\mathbf{g}}(\mathbf{x}) = -[\mathbf{A}(\mathbf{x}) - \mathbf{B}(\mathbf{x})\mathbf{R}^{-1}(\mathbf{x})\mathbf{B}'(\mathbf{x})\mathbf{P}(\mathbf{x})]'\mathbf{g}(\mathbf{x}) - \mathbf{C}'(\mathbf{x})\mathbf{Q}(\mathbf{x})\mathbf{z}(\mathbf{x}) \tag{3.2.10}$$

with the final condition

$$\mathbf{g}(\mathbf{x}, t_f) = \mathbf{C}'(t_f)\mathbf{F}\mathbf{z}(t_f) \tag{3.2.11}$$

The optimal state law of the nonlinear closed-loop optimal tracking state-dependent system can be obtained as

$$\dot{\mathbf{x}}(t) = [\mathbf{A}(\mathbf{x}) - \mathbf{B}(\mathbf{x})\mathbf{R}^{-1}(\mathbf{x})\mathbf{B}'(\mathbf{x})\mathbf{P}(\mathbf{x})]\mathbf{x}(t) + \mathbf{B}(\mathbf{x})\mathbf{R}^{-1}(\mathbf{x})\mathbf{B}'(\mathbf{x})\mathbf{g}(\mathbf{x}) \tag{3.2.12}$$

Similarly, an approximate analytic solution was developed based on the algebraic Riccati equation (ARE) to solve the differential Riccati equation (SDRE). The following procedure presents the steps of the solution for the finite-horizon differential

(SDRE) tracking problem[16]:

1. Calculating the steady state value $\mathbf{P_{ss}}(\mathbf{x})$ from an algebraic Riccati equation (ARE)

$$\mathbf{P_{ss}}(\mathbf{x})\mathbf{A}(\mathbf{x}) + \mathbf{A}'(\mathbf{x})\mathbf{P_{ss}}(\mathbf{x}) - \mathbf{P_{ss}}(\mathbf{x})\mathbf{B}(\mathbf{x})\mathbf{R}^{-1}(\mathbf{x})\mathbf{B}'(\mathbf{x})\mathbf{P_{ss}}(\mathbf{x}) + \mathbf{Q}(\mathbf{x}) = 0 \tag{3.2.13}$$

2. Applying a change-of-variables procedure and assuming

$$\mathbf{K}(\mathbf{x}, \mathbf{t}) = [\mathbf{P}(\mathbf{x}, \mathbf{t}) - \mathbf{P_{ss}}(\mathbf{x})]^{-1} \tag{3.2.14}$$

3. Calculating the closed-loop matrix $\mathbf{A_{cl}}(\mathbf{x})$ as

$$\mathbf{A_{cl}}(\mathbf{x}) = \mathbf{A}(\mathbf{x}) - \mathbf{B}(\mathbf{x})\mathbf{R^{-1}}\mathbf{B}'(\mathbf{x})\mathbf{P_{ss}}(\mathbf{x}) \tag{3.2.15}$$

4. Calculating $\mathbf{D}$ by solving the algebraic Lyapunov equation (ALE) [10]

$$\mathbf{A_{cl}}\mathbf{D} + \mathbf{D}\mathbf{A}'_{\mathbf{cl}} - \mathbf{B}\mathbf{R}^{-1}\mathbf{B}' = 0 \tag{3.2.16}$$

5. Solving the differential Lyapunov equation (DLE)

$$\dot{\mathbf{K}}(\mathbf{x}, t) = \mathbf{K}(\mathbf{x}, t)\mathbf{A}'_{\mathbf{cl}}(\mathbf{x}) + \mathbf{A_{cl}}(\mathbf{x})\mathbf{K}(\mathbf{x},t) - \mathbf{B}(\mathbf{x})\mathbf{R}^{-1}\mathbf{B}'(\mathbf{x}) \tag{3.2.17}$$

The solution of (3.2.17), as shown by [3], is given by

$$\mathbf{K}(\mathbf{x},t) = \mathbf{e}^{\mathbf{A_{cl}(t-t_f)}}(\mathbf{K}(\mathbf{x},t_f) - \mathbf{D})\mathbf{e}^{\mathbf{A_{cl}}'\mathbf{(t-t_f)}} + \mathbf{D} \tag{3.2.18}$$

6. Applying a change-of-variables procedure to obtain $\mathbf{P}(\mathbf{x},\mathbf{t})$ as

$$\mathbf{P}(\mathbf{x},t) = \mathbf{K}^{-1}(\mathbf{x},t) + \mathbf{P_{ss}}(t) \tag{3.2.19}$$

Calculating the steady state value $\mathbf{g_{ss}}(\mathbf{x})$ from the equation

$$\mathbf{g_{ss}}(\mathbf{x}) = [\mathbf{A}(\mathbf{x}) - \mathbf{B}(\mathbf{x})\mathbf{R}^{-1}(\mathbf{x})\mathbf{B}'(\mathbf{x})\mathbf{P_{ss}}(\mathbf{x})]'^{-1}\mathbf{C}'(\mathbf{x})\mathbf{Q}(\mathbf{x})\mathbf{z}(\mathbf{x}) \tag{3.2.20}$$

7. Applying a change-of-variables procedure and assume

$$\mathbf{K_g}(\mathbf{x},t) = [\mathbf{g}(\mathbf{x},t) - \mathbf{g_{ss}}(\mathbf{x})] \tag{3.2.21}$$

8. Solving the differential equation

$$\dot{\mathbf{K}}_\mathbf{g}(\mathbf{x},t) = -[\mathbf{A}(\mathbf{x}) - \mathbf{B}(\mathbf{x})\mathbf{R^{-1}}(\mathbf{x})\mathbf{B}'(\mathbf{x})\mathbf{P}(\mathbf{x},\mathbf{t})]'\mathbf{K_g}(\mathbf{x},\mathbf{t}) \tag{3.2.22}$$

The solution of (3.2.22) can be found as

$$\mathbf{K_g}(\mathbf{x},t) = \mathbf{e}^{-\mathbf{(A-BR^{-1}B'P)}'\mathbf{(t-t_f)}}[\mathbf{g}(\mathbf{x},t_f) - \mathbf{g_{ss}}(\mathbf{x})] \tag{3.2.23}$$

9. Applying a change-of-variables procedure and obtain $\mathbf{g}(\mathbf{x}, t)$

$$\mathbf{g}(\mathbf{x}, t) = \mathbf{K_g}(\mathbf{x}, t) + \mathbf{g_{ss}}(\mathbf{x}) \tag{3.2.24}$$

10. Thus, the optimal control input $\mathbf{u}(\mathbf{x}, t)$ is

$$\mathbf{u}(\mathbf{x}, t) = -\mathbf{R}^{-1}(\mathbf{x})\mathbf{B}'(\mathbf{x})[\mathbf{P}(\mathbf{x}, t)\mathbf{x}(t) - \mathbf{g}(\mathbf{x}, t)] \tag{3.2.25}$$

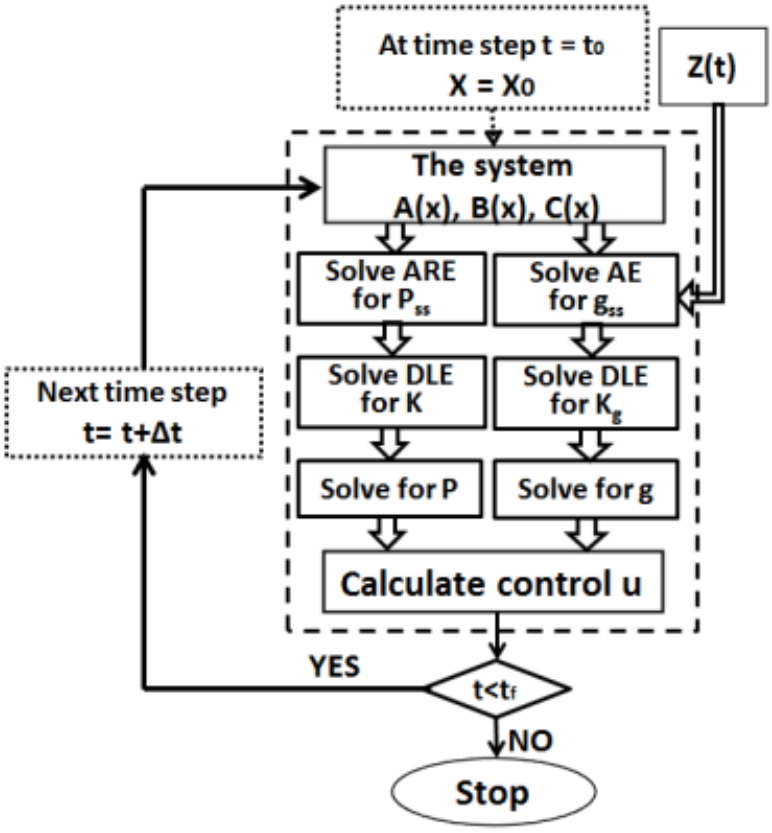

Figure 3.1: Flow Chart for Finite-Horizon Tracking with SDRE

Flow-chart in Figure 3.1 explains the whole procedure. The algorithm for finding

the control input $u(x,t)$ starts from an initial time, $t = t_0$ and iterates until a final time, $t = t_f$. In each iteration or in each time step Δt, the system goes through the 7 steps that are already descried. Generally, a final time denotes the time until when simulation should stop.

3.3 Soft Control Techniques

Rapid development in the field of soft control techniques had been seen in recent years. It is also called intelligent control systems. An intelligent control system is necessary for a very accurate modeling of a complex nonlinear system. Because it offers a reduction in modeling error with the help of control algorithms such as neural networks and fuzzy systems, it can model a controller when the system dynamic is not even properly known. So, fusion of soft control and hybrid control is extremely useful to model a very accurate control system [21], [6]. A fuzzy logic based controller for parallel hybrid electric vehicle was proposed by Khoucha and Benbouzid and Kheloui (2010). The PHEV required driving torque was generated by both ICE and induction motor (IM). They have used SOC of batteries and desired driving torque to design the controller with a view to reducing carbon-di-oxide emission and fuel economy [18].

A fusion of SC and HC control technique is used here to design a hybrid controller. The reference trajectory is generated from a S-type fuzzy membership function (MF). Then properly choosing values of Q and R and with applying the SDRE technique, a controller is designed.

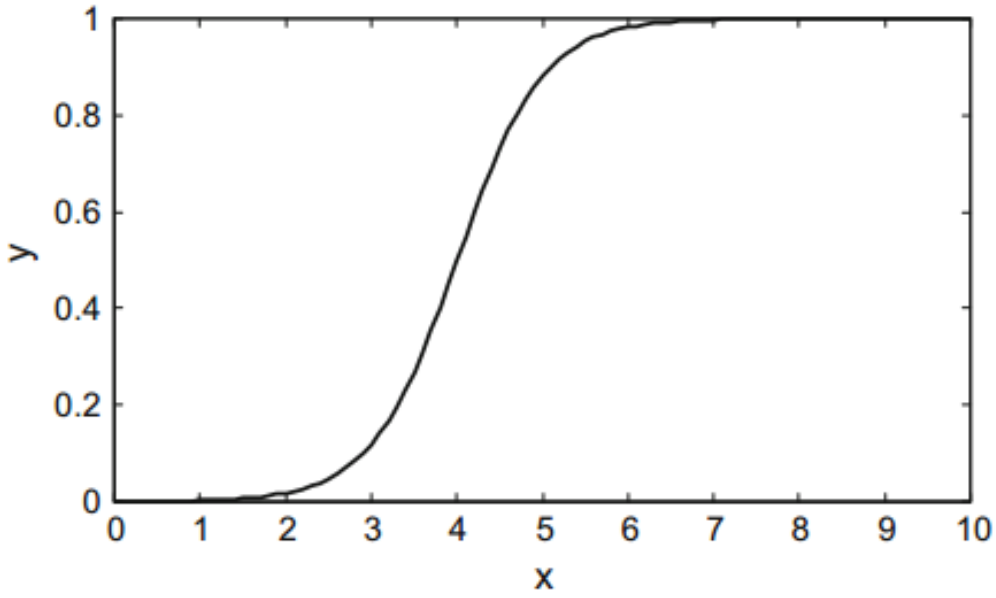

Figure 3.2: S-Type MF

3.3.1 Fuzzy Logic

The paper titled "Fuzzy Sets" [34] initiated fuzzy mathematics, a branch of mathematics that deals with vague, unclear and uncertainty of information. The uncertainty ranges from absolute true to absolute false. Fuzzy logic uses membership functions to characterize fuzziness of a variable. Out of six membership functions, S-type MF is chosen for designing a hybrid controller. A basic S-type function is shown in Figure 3.2.It shows a relationship between two variables. At the beginning, y coordinate has a smaller value and at the end, it steadies to a bigger coordinate. This scenario can be think of an EV battery charging, if SOC is considered at x-axis and battery voltage is considered at y-axis. The EV will come to the charging station with a low SOC value and will leave the station with a high SOC value.

$$f(x, a, c) = \frac{1}{1 + exp^{-a(x-c)}} \tag{3.3.1}$$

Chapter 4

MATLAB Simulation Results

This chapter discusses the simulation results. First, a nonlinear finite horizon tracking SDRE algorithm was compiled in MATLAB and then three reference voltages were chosen as reference voltages. The three reference voltages are

1. constant 5 volts for developing a controller with optimal control (Hard control, HC) techniques.

2. constant 12 volts for developing a controller with optimal control (Hard control, HC) techniques.

3. A reference voltage with the help of a fuzzy membership function for developing a controller with hybrid control (fusion of HC and SC) techniques.

4.1 Results for a Constant Voltage of 5 Volts

Consider, weighted matrices as

$$\mathbf{Q} = \begin{bmatrix} 10^{16} & 10^{14} & 10^{14} \\ 10^{14} & 10^{16} & 10^{14} \\ 10^{14} & 10^{14} & 10^{16} \end{bmatrix}$$

and

$$\mathbf{R} = \begin{bmatrix} 313000 \end{bmatrix};$$

The value of these weighted matrices plays a very important role, especially in tracking problems, where the goal of output is to follow a certain reference trajectory. Without a proper set of weighted matrix, usually there is always a deviation between the trajectories. Therefore, value of Q and R were chosen by trial and error process to achieve a best tracking scenario.

A constant 5-volts curve was selected as a charging profile. The profile was successfully tracked by the terminal voltage of the dual RC battery. The tracking controller had the terminal voltage settle to 5 volts before an initial spike, which occurred at the beginning of simulation and lasted for a few milliseconds. Figure 4.1 illustrates the tracking scenario obtained from a MATLAB simulation. In Figure 4.1(a) the deviation between the two curves is very negligible. Generally, error is calculated by this formula $error = reference - terminal$. Needless to say that this scenario is also depicted in Figure 4.1(b).

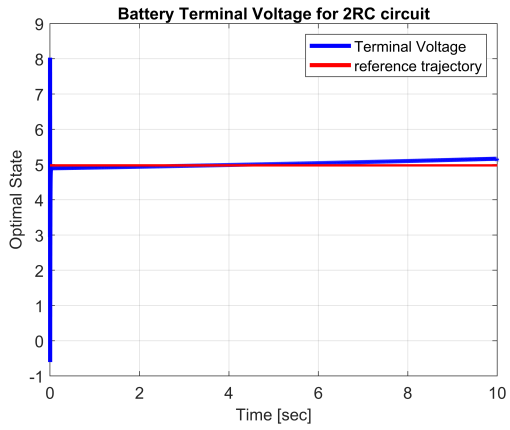

(a) Desired & Actual Trajectories for 5V Tracking

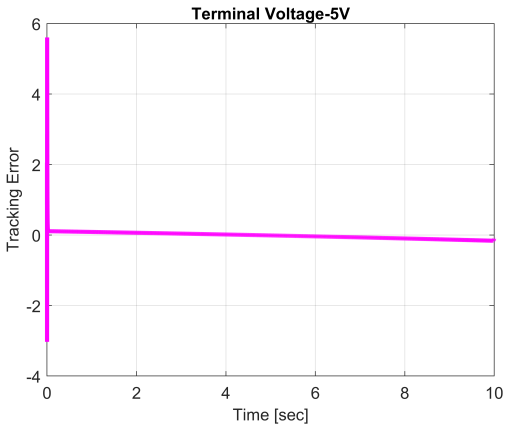

(b) Errors In 5V Tracking

Figure 4.1: Performance of 5V Tracking

4.2 Results for a Constant Voltage of 12 Volts

Again, the weighted matrices were chosen in a same way. Their values are-

$$\mathbf{Q} = \begin{bmatrix} 10^{16} & 10^{14} & 10^{14} \\ 10^{14} & 10^{16} & 10^{14} \\ 10^{14} & 10^{14} & 10^{16} \end{bmatrix}$$

and

$$\mathbf{R} = \begin{bmatrix} 5160000 \end{bmatrix};$$

A constant 12-volts curve was considered as a reference voltage. After the ephemeral overshoot the terminal voltage curve nearly caught up with the reference voltage. Figure 4.2 shows the simulation of first three seconds. In this time period, difference between the trajectories is little larger. However, the terminal voltage caught up with the reference voltage and showed a good tracking performance for the remaining 7 seconds. MATLAB simulation for tracking a 12 volt constant curve is

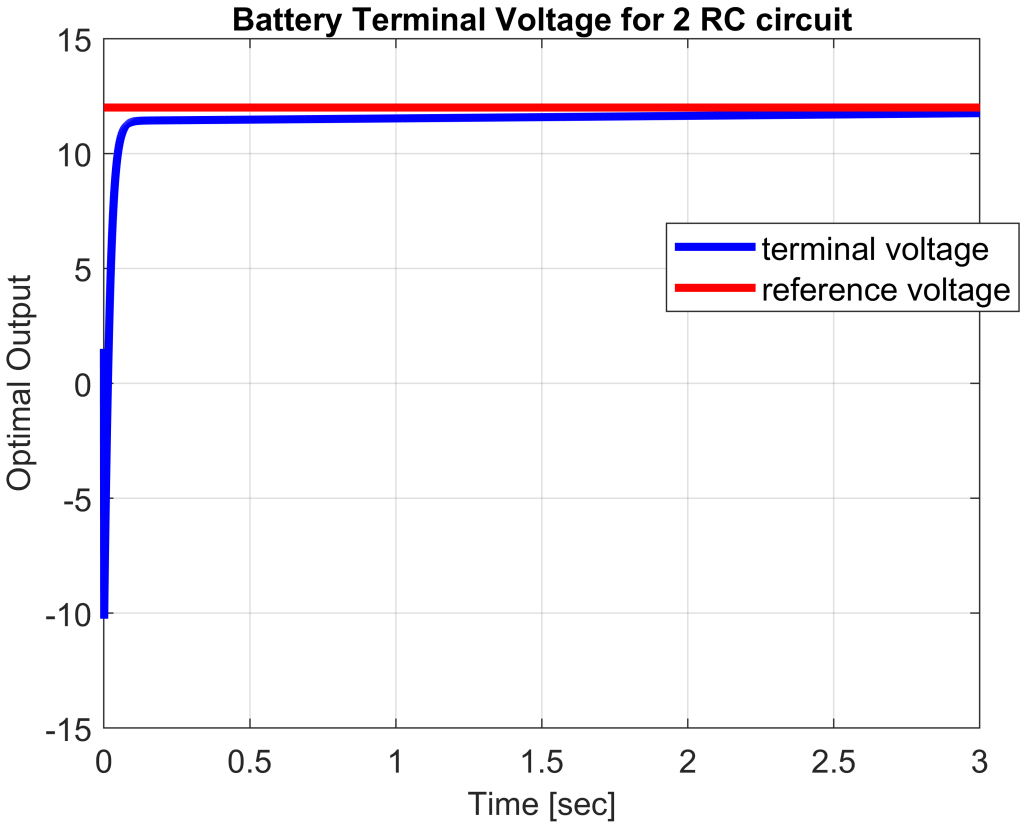

Figure 4.2: Initial Settling Time for 12V Tracking

illustrated in Figure 4.3(a) and 4.3(b). The error for this case is measured in a same way explained before.

4.3 Results with a Soft Control Technique

Consider, weighted matrices as

$$\mathbf{Q} = \begin{bmatrix} 10^{11.3} & 75^{5.3} & 75^{5.3} \\ 75^{5.3} & 10^{11.3} & 75^{5.3} \\ 75^{5.3} & 75^{5.3} & 10^{11.3} \end{bmatrix} * \mathbf{1.3540}$$

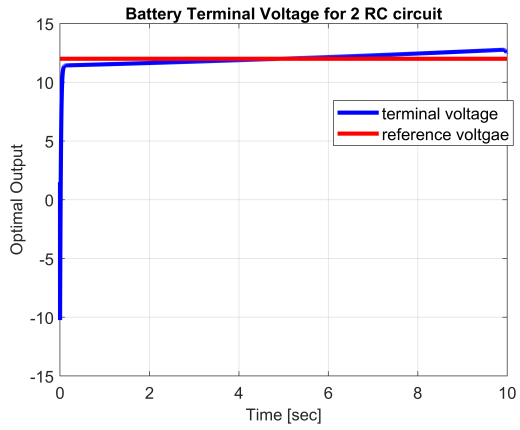

(a) Desired & Actual Trajectories for 12V TRACKING

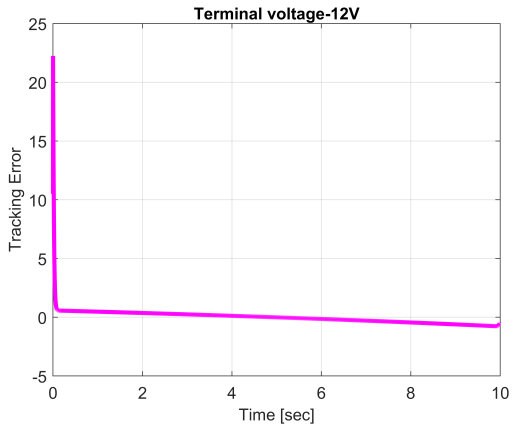

(b) Errors In 12V Tracking

Figure 4.3: Performance of 12V Tracking

and

$$\mathbf{R} = \left[291580\right];$$

The developed hybrid controller exhibited a significant tracking performance. The controller had the terminal voltage track a given trajectory, which was generated from a S-type fuzzy membership function. The trajectory started from a low value and gradually reached to 12V. The terminal voltage, with some errors tracked the reference voltage in a same way. The associated errors are small in margin and may be reduced with tuning the values of weighted matrices, Q and R. MATLAB simulation illustrates the tracking performance in Figure 4.4(a) and the associated tracking error is shown in the Figure 4.4(b).

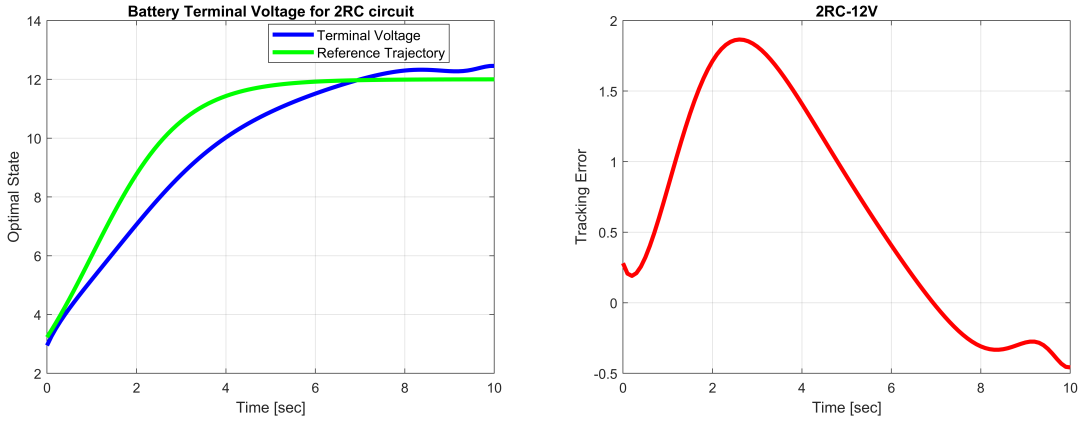

(a) Tracking a Fuzzy Function

(b) Associated Errors

Figure 4.4: Performance of Hybrid Control Tracking

Chapter 5

Conclusion and Future Work

5.1 Discussion and Conclusion

The tracking results suggest that a good tracking performance has been obtained overall. This control unit can be deployed in EVs for achieving smoother charging. Based on this work, a manuscript was also submitted for an IEEE conference. The title of the manuscript is "Advanced Tracking Strategies for Charging Electric Vehicle Batteries". The manuscript was prepared for the upcoming eleventh Conference on Innovative Smart Grid Technologies (ISGT 2020), sponsored by the IEEE Power Energy Society (PES), will be held on February 17-20, 2020 at the Grand Hyatt Washington, Washington DC.

5.2 Future Work

Since successful tracking was possible with 2-RC battery model this research can be continued to accomplish the following goals:

1. Finding an advanced finite-horizon nonlinear tracking strategy for a 3-RC Thevenin battery model. For its robustness, fast variation ability, a Thevenin model is most suitable for EV applications. Therefore, with SDRE technique, a SOC dependent tracking strategy development is one of the prime concerns.

2. The main idea behind fusin of hard and soft control technique is capturing the best features of a control mechanism. A fusion of hard and soft control technique with a 3-RC Thevenin model will be an one of its kind with ensuring maximum tracking ability hence producing optimal charging.

Appendix 1

Appendix 1 present MATLAB codes that were used in this thesis.

Codes for 5V tracking

```
clc;
clearvars;
x = [0.03;0.03;0.02];
    Q = [10^16 10^14 10^14; 10^14 10^16 10^14; 10^14 10^14
        10^16];
  R = 313000;
% C=[1 0 0;0 1 0;0 0 1];
tf=10;
Cuse=1;
F=eye(3);
Ptf = 1*eye(3);
Ztf = [0;0;0];
% gtf=C'*F*Ztf;
gtf=F*Ztf;
t = 0;
 h=1;
delta = 0.001;
      while ( t <tf )


I(h)=1;

Voc=-1.031*exp(-35*(x(3)))+3.685+0.2156*(x(3))-0.1178*(x(3))
    ^2+0.321*(x(3))^3;
Rs=0.1562*exp(-24.37*(x(3)))+0.07446;
R1=0.3208*exp(-29.14*(x(3)))+0.04669;
```

```
25 C1=-752.9*exp(-13.51*(x(3)))+703.6;
26 R2=6.603*exp(-155.2*(x(3)))+0.04984;
27 C2=-6056.6*exp(-27.12*(x(3)))+4475;
28  desired1(h)=5;
29 a11=-1/(R1*C1);
30 a22=-1/(R2*C2);
31 A = [a11 0 0; 0 a22 0; 0 0 0];
32
33 B=[(1/C1) (1/C2) -1/(Cuse*3600)]';
34 Pss = -care(-A,B,Q,R);
35
36          Ktf = inv(Ptf-Pss);
37          E= B*inv(R)*B';
38          Acl = A - E*Pss;
39          D = lyap(Acl,-E);
40          z = [desired1(h);desired1(h);0];
41          KK = expm(Acl*(t-tf))*(Ktf-D)*expm(Acl'*(t-tf)) +D;
42          Pe = inv(KK) + Pss;
43 %            gss = -inv(A - B*(inv(R))*B'*Pe)'*C'*Q*z;
44            gss = -inv(A - B*(inv(R))*B'*Pe)'*Q*z;
45          AA = A - B*inv(R)*B'*Pe;
46          BB = B*inv(R)*B';
47          Kg = expm((A-AA)'*(t-tf))*(gtf-gss);
48          ge =    gss + Kg;
49          xdot = AA*x + BB*ge;
50
51          control_u = -inv(R)*B'*(Pe*x - ge);
```

```
52          state1(h)=x(1);
53          state2(h)=x(2);
54         output(h)=Voc-state1(h)-state2(h)-Rs*I(h);
55
56
57          d_c(h) = control_u(1);
58          error(h) = desired1(h) - output(h);
59
60          x =x+delta *xdot;
61          h=h+1
62          t = t + delta;
63
64          h_end = h;
65
66
67      end
68
69
70 t = (0:delta:tf);
71 if (tf<5  || tf>18)
72      t = (delta:delta:tf);
73 end
74  % Optimal Control
75  figure;box; hold on; grid on;
76  xlabel('Time [sec]'); ylabel('Optimal Control')
77 % axis([0 10 -10^132 0])
78  plot(t,d_c,'LineWidth',3)
```

```
79
80 figure
81 plot(t,I,'g','Linewidth',3)
82 title('Input Current')
83 xlabel('time')
84 grid on
85
86
87 figure;box;  hold on; grid on;
88 title('Battery Terminal Voltage for 2RC circuit')
89 xlabel('Time [sec]'); ylabel('Optimal State');
90 plot(t,output,'b','Linewidth',3)
91 plot(t,desired1,'r','LineWidth',3);
92
93 figure;box; hold on; grid on;
94 title('2RC-5V')
95 xlabel('Time [sec]'); ylabel('Tracking Error');
96 plot(t,error,'m','LineWidth',3)
```

Codes for 12V tracking

```
clc;
clearvars;
x = [0;0;0];
%     Q = [10^15.9 0 0; 0 10^15.9 0; 0 0 10^15.9]; % 3-by-3
%     Q = [10^-9 10^-9 10^-9; 10^-9 10^-9 10^-9; 10^-9 10^-9
    10^-9];
      Q = [10^16 10^14 10^14; 10^14 10^16 10^14; 10^14 10^14
          10^16];

%    R=1e10;
   R = 516*10000;


tf=10;
Cuse=1;
F=eye(3);
Ptf = 1*eye(3);
Ztf = [0;0;0];
gtf=F*Ztf;
t = 0;
 h=1;
delta = 0.001;
       while ( t <tf )


%   I(h)=square(2*pi*(0.25)*t);
```

```
25  I(h)=5;
26
27
28 Voc=-1.031*exp(-35*(x(3)))+3.685+0.2156*(x(3))-0.1178*(x(3))
       ^2+0.321*(x(3))^3;
29 Rs=0.1562*exp(-24.37*(x(3)))+0.07446;
30 R1=0.3208*exp(-29.14*(x(3)))+0.04669;
31 C1=-752.9*exp(-13.51*(x(3)))+703.6;
32 R2=6.603*exp(-155.2*(x(3)))+0.04984;
33 C2=-6056.6*exp(-27.12*(x(3)))+4475;
34  desired(h)=12;
35 % desired1(h)=square(2*pi*(0.25)*t);
36
37 a11=-1/(R1*C1);
38 a22=-1/(R2*C2);
39 A = [a11 0 0; 0 a22 0; 0 0 0]; % 3-by-3 A(x) for Uzun Model
40 %   A = [(-1/(R1*C1))  0;0 (-1/(R2*C2)) ;];          % 2-by
       -2 A(x) for Uzun Model
41 % A=-A;
42 B=[(1/C1) (1/C2) -1/(1*3600)]'; % 3-by-1 B(x) for Uzun Model
43
44 Pss = -care(-A,B,Q,R);
45
46 %          [K,P,e] = lqr(A,B,Q,R);
47 %          Pss = P;
48 %
49          Ktf = inv(Ptf-Pss);
```

```
50          E= B*inv(R)*B';
51          Acl = A - E*Pss;
52          D = lyap(Acl,-E);
53          z = [desired(h);desired(h);0];
54 %
55          KK = expm(Acl*(t-tf))*(Ktf-D)*expm(Acl'*(t-tf)) +D;
56 %            Ztf = [0;0;0];
57 %            gtf=C'*F*Ztf;
58          Pe = inv(KK) + Pss;
59 %            gss = -inv(A - B*(inv(R))*B'*Pe)'*C'*Q*z;
60            gss = -inv(A - B*(inv(R))*B'*Pe)'*Q*z;
61          AA = A - B*inv(R)*B'*Pe;
62          BB = B*inv(R)*B';
63          Kg = expm((A-AA)'*(t-tf))*(gtf-gss);
64          ge =    gss + Kg;
65          xdot = AA*x + BB*ge;
66
67
68          control_u = -inv(R)*B'*(Pe*x - ge);
69          state1(h)=x(1);
70          state2(h)=x(2);
71         output(h)=Voc-state1(h)-state2(h)-Rs*I(h);
72
73
74          d_c(h) = control_u(1);
75          error(h) = desired(h) - output(h);
76
```

```
77          x =x+delta *xdot;
78          h=h+1
79          t = t + delta;
80
81          h_end = h;
82
83
84      end
85
86
87 t = (0:delta:tf);
88 if (tf<5   ||  tf>18)
89      t = (delta:delta:tf);
90 end
91
92 % plot(t,desired)
93
94 % figure
95 % plot(t,I,'g','Linewidth',3)
96 % title('Input Current')
97 % xlabel('time')
98 % ylabel('Current(A)')
99 % grid on
100 %
101 % figure
102 % plot(t,desired,'b','Linewidth',3)
103 % title('Desired Trajectory')
```

```
104 % xlabel('time')
105 % ylabel('Voltage(V)')
106 % grid on
107 %
108 %% Optimal Control
109 figure;box; hold on; grid on;
110 xlabel('Time [sec]'); ylabel('Optimal Control')
111 % axis([0 10 -10^132 0])
112 plot(t,d_c,'LineWidth',3)
113
114 figure;box;  hold on; grid on;
115 title('Battery Terminal Voltage for 2 RC circuit')
116 xlabel('Time [sec]'); ylabel('Optimal Output');
117 plot(t,output,'b','Linewidth',3)
118 plot(t,desired,'r','LineWidth',3);
119
120
121
122 figure;box;  hold on; grid on;
123 title('Battery Terminal Voltage for 2 RC circuit')
124 xlabel('Time [sec]'); ylabel('Optimal Output');
125 axis([0 1 -15 15])
126 % plot(t,output,t,desired,'LineWidth',3);
127 plot(t,output,'b','Linewidth',3)
128 plot(t,desired,'r','LineWidth',3);
129
130 figure;box;  hold on; grid on;
```

```
131 title('Battery Terminal Voltage for 2 RC circuit')
132 xlabel('Time [sec]'); ylabel('Optimal Output');
133 axis([0 3 -15 15])
134 % plot(t,output,t,desired,'LineWidth',3);
135 plot(t,output,'b','Linewidth',3)
136 plot(t,desired,'r','LineWidth',3);
137
138 figure;box;  hold on; grid on;
139 title('Battery Terminal Voltage for 2 RC circuit')
140 xlabel('Time [sec]'); ylabel('Optimal Output');
141 axis([1 3 -15 15])
142 % plot(t,output,t,desired,'LineWidth',3);
143 plot(t,output,'b','Linewidth',3)
144 plot(t,desired,'r','LineWidth',3);
145
146 figure;box; hold on; grid on;
147 xlabel('Time [sec]'); ylabel('Tracking Error');
148 title('Terminal voltage-12V')
149 %% axis([0 10 -10^132 0])
150 %  plot(t(1:10),error(1:10),'m-.','LineWidth',3);
151 plot(t,error,'m','LineWidth',3)
152
153 mean(error)
154
155 % figure;box; hold on; grid on;
156 % xlabel('Time [sec]'); ylabel('Tracking Error');
157 %%% axis([0 10 -10^132 0])
```

```
158 %% plot(t(1:10),error(1:10),'m-.','LineWidth',3);
159 % plot(t,error,'m','LineWidth',3)
```

Codes for 12V fuzzy control technique

```
clc;
clearvars;
x = [0.03;0.03;0.3];
%  Q = 4*[10^11.3  75^5.3  75^5.3; 75^5.3  10^11.3  75^5.3;
    75^5.3  75^5.3  10^11.3]; %locked pair a
%   R = 0.856*456342; %locked pair a
Q = 27.45*[10^11.3  75^5.3  75^5.3; 75^5.3  10^11.3  75^5.3;
    75^5.3  75^5.3  10^11.3]*0.03;
R = 0.433*678904;
% C=[1  0  0;0  1  0;0  0  1];
tf=10;
Cuse=1;
F=eye(3);
Ptf = 10*eye(3);
Ztf = [0;0;0];
% gtf=C'*F*Ztf;
gtf=F*Ztf;
t = 0;
 h=1;
delta = 0.1;
      while ( t <tf )


I(h)=5;

Voc=-1.031*exp(-35*(x(3)))+3.685+0.2156*(x(3))-0.1178*(x(3))
```

```
    ^2+0.321*(x(3))^3;
Rs=0.1562*exp(-24.37*(x(3)))+0.07446;
R1=0.3208*exp(-29.14*(x(3)))+0.04669;
C1=-752.9*exp(-13.51*(x(3)))+703.6;
R2=6.603*exp(-155.2*(x(3)))+0.04984;
C2=-6056.6*exp(-27.12*(x(3)))+4475;


% desired1(h)=5;
ref=sigmf(t,[1  1.0001]);
% ref=sigmf(t,[3  5]);
ref=12*ref;
desired1(h)=ref;


a11=-1/(R1*C1);
a22=-1/(R2*C2);
A = [a11  0  0; 0  a22  0; 0  0  0];

B=[(1/C1)  (1/C2)  -1/(Cuse*3600)]';
Pss = -care(-A,B,Q,R);
Ktf = inv(Ptf-Pss);
E= B*inv(R)*B';
Acl = A - E*Pss;
D = lyap(Acl,-E);
z = [desired1(h);desired1(h);0];
KK = expm(Acl*(t-tf))*(Ktf-D)*expm(Acl'*(t-tf)) +D;
```

```
51 Pe = inv(KK) + Pss;
52 gss = -inv(A - B*(inv(R))*B'*Pe)'*Q*z;
53 AA = A - B*inv(R)*B'*Pe;
54 BB = B*inv(R)*B';
55 Kg = expm((A-AA)'*(t-tf))*(gtf-gss);
56 ge =    gss + Kg;
57 xdot = AA*x + BB*ge;
58 control_u = -inv(R)*B'*(Pe*x - ge);
59 state1(h)=x(1);
60 state2(h)=x(2);
61 output(h)=Voc-state1(h)-state2(h)-Rs*I(h);
62 d_c(h) = control_u(1);
63 error(h) = desired1(h) - output(h);
64 x =x+delta *xdot;
65 h=h+1
66 t = t + delta;
67 h_end = h;
68
69
70       end
71
72
73 t = (0:delta:tf);
74 if (tf<5   ||  tf>18)
75      t = (delta:delta:tf);
76 end
77  % Optimal Control
```

```
78 %  figure;box; hold on; grid on;
79 %  xlabel('Time [sec]'); ylabel('Optimal Control')
80 %% axis([0 10 -10^132 0])
81 %  plot(t,d_c,'LineWidth',3)
82 %
83 % figure
84 % plot(t,I,'g','Linewidth',3)
85 % title('Input Current')
86 % xlabel('time')
87 % grid on
88
89
90 figure;box;  hold on; grid on;
91 title('Battery Terminal Voltage for 2RC circuit')
92 xlabel('Time [sec]'); ylabel('Optimal State');
93 plot(t,output,'b','Linewidth',3)
94 plot(t,desired1,'g','LineWidth',3);
95
96 figure;box; hold on; grid on;
97 title('2RC-12V')
98 xlabel('Time [sec]'); ylabel('Tracking Error');
99 plot(t,error,'r','LineWidth',3)
100 mean(error)
```

Appendix 2

Appendix 2 presents a manuscript that was submitted at a Conference on Innovative Smart Grid Technologies (ISGT 2020), sponsored by the IEEE Power Energy Society (PES), will be held on February 17-20, 2020 at the Grand Hyatt Washington, Washington DC. The title of the manuscript is **Advanced Tracking Strategies for Charging Electric Vehicle Batteries**. The manuscript was authored by- (1) Murtaza Kamal Pasha Khan, *Dept. of Electrical Engineering, University of Minnesota Duluth*, Duluth, USA. (2) D. Subbaram Naidu, Fellow, IEEE, *Dept. of Electrical Engineering, University of Minnesota Duluth*, Duluth, USA and (3) Ona Egbue, PhD, CPEM, *Dept. of Informatics and Engineering Systems, University of South Carolina Upstate*, Spartanburg, USA.

Advanced Tracking Strategies for Charging Electric Vehicle Batteries

***Abstract*-Challenges and opportunities of integrating electric vehicles (EV) with an electric grid have been of great interest for the past few years. In order to integrate with an electric grid, a battery model of the EV should have adequate control mechanisms. In this paper, we consider a nonlinear model of a 2-RC battery. For optimal tracking of a reference trajectory, a closed-loop optimal control is obtained by using the State-Dependent Riccati Equation (SDRE) technique with performance index to minimize the quadratic error between the reference and actual trajectories. Simulation results with a lithium-ion (li-ion) battery shows good tracking performance.**

***Index Terms*-Nonlinear EV battery model, Charging, Closed-loop optimal control, State dependent Riccati equation (SDRE).**

I Introduction

Battery modeling for an electric vehicle is very important factor. A properly balanced battery model assures safe charging/discharging techniques and optimal usage of batteries. Therefore, recent studies have focused on developing updated battery models. For example, one study proposed a single RC equivalent battery model to represent the short term and long-term battery dynamics under consideration of the Battery Management System (BMS) [2]. A comparative study showed that having more parallel branches of RC circuit tends to increase the accuracy of the model, while it is also true that more branches complicates the mathematical modeling and need more look-up tables[22]. The study also shows that electrical equivalent circuit model (EECM), which uses lumped electrical components to represent dynamic behaviors of a li-ion battery cell is better than the other models. Such as EECM has low complexity, high interpretability and used for the state-of-charge (SOC) and real-time control applications [3].

An optimal control system aims to provide the best solution for a given problem. The best solution comes by following a trajectory or by reaching a target. Applications of optimal control can be found in different fields such as electrical power, aerospace, chemical plants and biology. A prominent method used for designing a nonlinear optimal controller is the state dependent Riccati equation (SDRE). Recently SDRE technique has been applied to solve wind energy problems and control of a robotic hand [15],[17],[24]. This group of researchers have designed a non-linear observer for estimating the state of charge (SOC) and state of health (SOH) parameters of non-linear li-ion batteries with the SDRE technique. However, they do not address the tracking strategy of battery terminal voltage [1]. Research has been carried out in some other aspects of a li-ion battery model, although, none of these researches develop any method to combine a battery model with optimal control technique.

In this paper, a novel combination of EECM and SDRE technique is shown to develop an optimal controller. The SDRE technique is applied to track the terminal voltage of an EV battery cell. The electrical battery model depends on the SOC, therefore a non-linear state-space dynamic system is formed and solved as a finite-horizon, closed-loop, optimal tracking problem. The SDRE technique converts this system to a linear differential Lyapunov equation and solves it to find the optimal control.

The organization of this paper is as follows: Section II discusses the battery modeling, Section III describes the optimal control technique, Section IV discusses the simulation results, and Section V provides a conclusion for the paper.

II Battery Modeling

A second-order RC (2 RC) (shown in Figure 1) EECM with nonlinear dynamic equations is used to investigate the output or terminal characteristics of a lithium-ion (li-ion) battery under different charging/discharging and temperature conditions. This dual RC model is considered for its good balance between complexity and accuracy. The circuit model consists of R_0, R_1, C_1, R_2 and C_2, where R_0 indicates the instantaneous voltage drop of the battery terminal voltage, and the RC networks expresses the long-term and short-term transient behavior of the battery and all the elements are SOC dependent. Dynamic equations of the circuit elements are given below [9],[25],[29],[28].

$$\begin{aligned} V_{OC}(SOC) = &- 1.031.exp^{-35*SOC} + 3.685 + 0.2156 * SOC \\ &- 0.1178 * SOC^2 + 0.3201 * SOC^3 \end{aligned} \tag{II.2}$$

$$R_0(SOC) = -0.1562.exp^{-24.37*SOC} + 0.07446 \tag{II.3}$$

$$R_1(SOC) = -0.3208.exp^{-29.14*SOC} + 0.04669 \tag{II.4}$$

$$C_1(SOC) = -752.9exp^{-13.51*SOC} + 703.6 \tag{II.5}$$

$$R_2(SOC) = -6.603.exp^{-155.2*SOC} + 0.04984 \tag{II.6}$$

$$C_2(SOC) = -6056.exp^{-27.12*SOC} + 4475 \tag{II.7}$$

a. Battery State-Space Model

The dynamics of this dual RC model can also be expressed in state-space form, which is also in a desired state dependent coefficient (SDC) form for this battery model. An appropriate SDC form of a nonlinear model makes it controllable or at least stabilizable. Hence, expressing it in a SDC form is very crucial for optimal control applications. Here

$$\dot{x}(t) = Ax(t) + Bu(t)$$

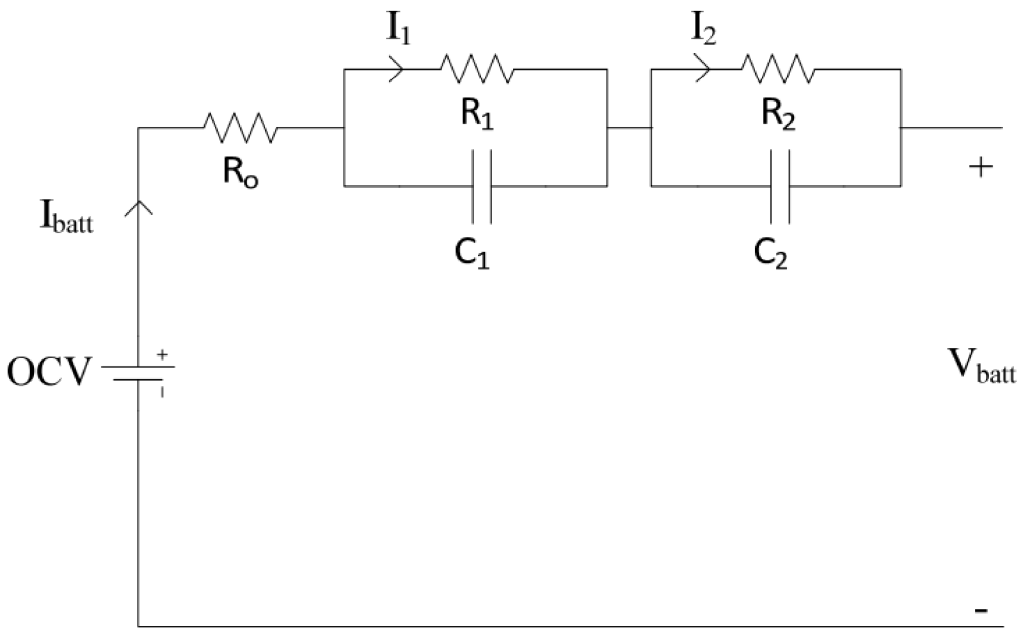

Figure 1: 2-RC branched battery model

is a desired SDC form of this system. And the parameters $A(x)$ and $B(x)$ are

$$\mathbf{A}(\mathbf{x}) = \begin{bmatrix} A_{11} & 0 & 0 \\ 0 & A_{22} & 0 \\ 0 & 0 & 0 \end{bmatrix}$$

and,

$$\mathbf{B}(\mathbf{x}) = \begin{bmatrix} B_{11} \\ B_{21} \\ B_{31} \end{bmatrix}$$

where,

$$A_{11} = \frac{-1}{R_1(SOC)C_1(SOC)},$$
$$A_{22} = \frac{-1}{R_2(SOC)C_2(SOC)},$$
$$B_{11} = \frac{1}{C_1(SOC)},$$
$$B_{21} = \frac{1}{C_2(SOC)},$$
$$and$$
$$B_{31} = \frac{-\eta}{Q},$$

Here, η represents coulombic efficiency (energy loss) of the battery. It is assumed to be 1 for this study . Q, a constant, expresses total capacity or maximum coulomb hours of a battery. The input of this circuit $u(t) = I(t)$, is a constant current and the output equation of the battery/terminal voltage equation of the battery can be expressed as

$$y(t) = V_{batt} = V_{OC}(SOC) - V_1(SOC) - V_2(SOC) - R_0(SOC).I(t), \tag{II.8}$$

V_1 and V_2 is calculated by applying Kirchoff's law,

$$\dot{V_1}(SOC) = \frac{-V_1(SOC)}{R_1(SOC)C_1(SOC)} + \frac{u(t)}{C_1(SOC)}, \tag{II.9}$$

$$\dot{V}_2(SOC) = \frac{-V_2(SOC)}{R_2(SOC)C_2(SOC)} + \frac{u(t)}{C_2(SOC)} \tag{II.10}$$

III Optimal Control Technique

In this section, the control technique applied on the EV battery model is explained. We are considering a finite horizon non-linear deterministic system. This section shows a step-by-step approach for developing the nonlinear system and obtaining a solution for the above case.

a. Finite Horizon Non-linear Tracking System

Suppose, the nonlinear system is,

$$\dot{\mathbf{x}}(t) = \mathbf{f}(\mathbf{x}) + \mathbf{g}(\mathbf{x})\mathbf{u}(t), \tag{III.1}$$

$$\mathbf{y}(t) = \mathbf{h}(\mathbf{x}). \tag{III.2}$$

The nonlinear is transformed into a linear-like structure, which termed as state dependent coefficient (SDC) form

$$\dot{\mathbf{x}}(t) = \mathbf{A}(\mathbf{x})\mathbf{x}(t) + \mathbf{B}(\mathbf{x})\mathbf{u}(t), \tag{III.3}$$

$$\mathbf{y}(t) = \mathbf{C}(\mathbf{x})\mathbf{x}(t). \tag{III.4}$$

where, $\mathbf{f}(\mathbf{x}) = \mathbf{A}(\mathbf{x})\mathbf{x}(t)$, $\mathbf{B}(\mathbf{x})= \mathbf{g}(\mathbf{x})$, and $\mathbf{h}(\mathbf{x}) = \mathbf{C}(\mathbf{x})\mathbf{x}(t)$.

The goal is to obtain a state feedback optimal control of the form $\mathbf{u}(\mathbf{x},t) =$

$-\mathbf{K}(\mathbf{x},t)\mathbf{x}(t)$, which minimizes a cost function[23]

$$\mathbf{J}(\mathbf{x},\mathbf{u}) = \frac{1}{2}\mathbf{x}'(t_f)\mathbf{F}\mathbf{x}(t_f)+ \\ \frac{1}{2}\int_{t_0}^{t_f} [\mathbf{x}'(t)\mathbf{Q}(\mathbf{x})\mathbf{x}(t) + \mathbf{u}'(\mathbf{x})\mathbf{R}(\mathbf{x})\mathbf{u}(\mathbf{x})]\ dt, \tag{III.5}$$

$\mathbf{Q}(\mathbf{x})$ is called error weighted matrix. In order to keep the error $\mathbf{e}(\mathbf{t})$ small and error squared non-negative, $\mathbf{Q}(\mathbf{x})$ must be *positive semi-definite* matrices. For the same purpose, the other requirements should be fulfilled. Such as $\mathbf{F}$ should be symmetric and *positive semi-definite* matrix, and the control weighted matrix, $\mathbf{R}(\mathbf{x})$ must be symmetric *positive definite*. $\mathbf{x}'(t)\mathbf{Q}(\mathbf{x})\mathbf{x}(t)$ is a measure of state accuracy and $\mathbf{u}'(\mathbf{x})\mathbf{R}(\mathbf{x})\mathbf{u}(\mathbf{x})$ is a measure of control effort.

Consider the given nonlinear state-dependent system (III.3) and (III.4), here $\mathbf{z}(t)$ is the *desired* output or trajectory,where the closed-loop error is $\mathbf{e}(t) = \mathbf{z}(t) - \mathbf{y}(t)$.

b. Solution for Finite-Horizon Tracking Problem using SDRE and Vector Differential Equation (VDE)

The optimal closed-loop control input is given as

$$\mathbf{u}(\mathbf{x}) = -\mathbf{R}^{-1}\mathbf{B}'(\mathbf{x})[\mathbf{P}(\mathbf{x})\mathbf{x} - \mathbf{g}(\mathbf{x})] \tag{III.6}$$

where $\mathbf{P}(\mathbf{x})$, is symmetric and positive-definite, and is the solution of the differ-

ential Riccati equation (SDRE) that is given by

$$-\dot{\mathbf{P}}(\mathbf{x}) = \mathbf{P}(\mathbf{x})\mathbf{A}(\mathbf{x}) + \mathbf{A}'(\mathbf{x})\mathbf{P}(\mathbf{x}) - \mathbf{P}(\mathbf{x})\mathbf{B}(\mathbf{x})\mathbf{R}^{-1}\mathbf{B}'(\mathbf{x})\mathbf{P}(\mathbf{x}) + \mathbf{C}'(\mathbf{x})\mathbf{Q}(\mathbf{x})\mathbf{C}(\mathbf{x}) \quad \text{(III.7)}$$

with the final condition

$$\mathbf{P}(\mathbf{x}, t_f) = \mathbf{C}'(t_f)\mathbf{F}\mathbf{C}(t_f) \quad \text{(III.8)}$$

and $\mathbf{g}(\mathbf{x})$ is a solution of the state-dependent non-homogeneous vector differential equation (VDE) which has the form

$$\dot{\mathbf{g}}(\mathbf{x}) = -[\mathbf{A}(\mathbf{x}) - \mathbf{B}(\mathbf{x})\mathbf{R}^{-1}(\mathbf{x})\mathbf{B}'(\mathbf{x})\mathbf{P}(\mathbf{x})]'\mathbf{g}(\mathbf{x}) - \mathbf{C}'(\mathbf{x})\mathbf{Q}(\mathbf{x})\mathbf{z}(\mathbf{x}) \quad \text{(III.9)}$$

with the final condition

$$\mathbf{g}(\mathbf{x}, t_f) = \mathbf{C}'(t_f)\mathbf{F}\mathbf{z}(t_f) \quad \text{(III.10)}$$

The optimal state law of the nonlinear closed-loop optimal tracking state-dependent system can be obtained as

$$\dot{\mathbf{x}}(\mathbf{t}) = [\mathbf{A}(\mathbf{x}) - \mathbf{B}(\mathbf{x})\mathbf{R}^{-1}(\mathbf{x})\mathbf{B}'(\mathbf{x})\mathbf{P}(\mathbf{x})]\mathbf{x}(\mathbf{t}) + \mathbf{B}(\mathbf{x})\mathbf{R}^{-1}(\mathbf{x})\mathbf{B}'(\mathbf{x})\mathbf{g}(\mathbf{x}) \quad \text{(III.11)}$$

Similarly, an approximate analytic solution was developed based on the algebraic Riccati equation (ARE) to solve the differential Riccati equation (SDRE). The following procedure presents the steps of the solution for the finite-horizon differential

(SDRE) tracking problem[16]:

1. Calculating the steady state value $\mathbf{P_{ss}(x)}$ from an algebraic Riccati equation (ARE)

$$\mathbf{P_{ss}(x)A(x)} + \mathbf{A'(x)P_{ss}(x)} - \mathbf{P_{ss}(x)B(x)R^{-1}(x)B'(x)P_{ss}(x)} + \mathbf{Q(x)} = 0 \tag{III.12}$$

2. Applying a change-of-variables procedure and assuming

$$\mathbf{K(x,t)} = [\mathbf{P(x,t)} - \mathbf{P_{ss}(x)}]^{-1} \tag{III.13}$$

3. Calculating the closed-loop matrix $\mathbf{A_{cl}(x)}$ as

$$\mathbf{A_{cl}(x)} = \mathbf{A(x)} - \mathbf{B(x)R^{-1}B'(x)P_{ss}(x)} \tag{III.14}$$

4. Calculating $\mathbf{D}$ by solving the algebraic Lyapunov equation[10]

$$\mathbf{A_{cl}D} + \mathbf{DA'_{cl}} - \mathbf{BR^{-1}B'} = 0 \tag{III.15}$$

5. Solving the differential Lyapunov equation

$$\dot{\mathbf{K}}\mathbf{(x,t)} = \mathbf{K(x,t)A'_{cl}(x)} + \mathbf{A_{cl}(x)K(x,}t\mathbf{)} - \mathbf{B(x)R^{-1}B'(x)} \tag{III.16}$$

The solution of (III.16), as shown by[3], is given by

$$\mathbf{K}(\mathbf{x},\mathbf{t}) = \mathbf{e}^{\mathbf{A_{cl}(t-t_f)}}(\mathbf{K}(\mathbf{x},t_f) - \mathbf{D})\mathbf{e}^{\mathbf{A_{cl}}'\mathbf{(t-t_f)}} + \mathbf{D} \tag{III.17}$$

6. Applying a change-of-variables procedure to obtain $\mathbf{P}(\mathbf{x},\mathbf{t})$ as

$$\mathbf{P}(\mathbf{x},t) = \mathbf{K}^{-1}(\mathbf{x},t) + \mathbf{P_{ss}}(t) \tag{III.18}$$

Calculating the steady state value $\mathbf{g_{ss}}(\mathbf{x})$ from the equation

$$\mathbf{g_{ss}}(\mathbf{x}) = [\mathbf{A}(\mathbf{x}) - \mathbf{B}(\mathbf{x})\mathbf{R}^{-1}(\mathbf{x})\mathbf{B}'(\mathbf{x})\mathbf{P_{ss}}(\mathbf{x})]'^{-1}\mathbf{C}'(\mathbf{x})\mathbf{Q}(\mathbf{x})\mathbf{z}(\mathbf{x}) \tag{III.19}$$

7. Applying a change-of-variables procedure and assume

$$\mathbf{K_g}(\mathbf{x},t) = [\mathbf{g}(\mathbf{x},t) - \mathbf{g_{ss}}(\mathbf{x})] \tag{III.20}$$

8. Solving the differential equation

$$\dot{\mathbf{K}}_\mathbf{g}(\mathbf{x},\mathbf{t}) = -[\mathbf{A}(\mathbf{x}) - \mathbf{B}(\mathbf{x})\mathbf{R^{-1}}(\mathbf{x})\mathbf{B}'(\mathbf{x})\mathbf{P}(\mathbf{x},\mathbf{t})]'\mathbf{K_g}(\mathbf{x},\mathbf{t}) \tag{III.21}$$

The solution of (III.21) can be found as

$$\mathbf{K_g}(\mathbf{x},\mathbf{t}) = \mathbf{e}^{-\mathbf{(A-BR^{-1}B'P)}'\mathbf{(t-t_f)}}[\mathbf{g}(\mathbf{x},\mathbf{t_f}) - \mathbf{g_{ss}}(\mathbf{x})] \tag{III.22}$$

9. Applying a change-of-variables procedure to obtain $\mathbf{g}(\mathbf{x}, \mathbf{t})$

$$\mathbf{g}(\mathbf{x}, \mathbf{t}) = \mathbf{K_g}(\mathbf{x}, \mathbf{t}) + \mathbf{g_{ss}}(\mathbf{x}) \tag{III.23}$$

10. Thus, the optimal control input $\mathbf{u}(\mathbf{x}, \mathbf{t})$ is

$$\mathbf{u}(\mathbf{x}, \mathbf{t}) = -\mathbf{R}^{-1}(\mathbf{x})\mathbf{B}'(\mathbf{x})[\mathbf{P}(\mathbf{x}, \mathbf{t})\mathbf{x}(\mathbf{t}) - \mathbf{g}(\mathbf{x}, \mathbf{t})] \tag{III.24}$$

IV Simulations and Results

In this section, simulation results of the tracking problems are provided. Simulations were performed for 10 seconds by MATLAB. To imitate the real charging scenario of an electric vehicle, constant voltages of 5 volts and 12 volts were selected as reference trajectories. As already stated, a dual RC EECM of a li-ion battery was analyzed for the optimal result. Parameters such as values of Q and R are tuned in order to minimize tracking error.

a. Results for 5 Volts Tracking

A constant 5-volts curve was selected as a charging profile. The profile was successfully tracked by the terminal voltage of the battery. The HC tracking controller has the terminal voltage settle to 5 volts before an initial spike, which occurred at the beginning of simulation and lasted for a few milliseconds. Figure 2 illustrates the tracking scenario obtained from MATLAB simulation.

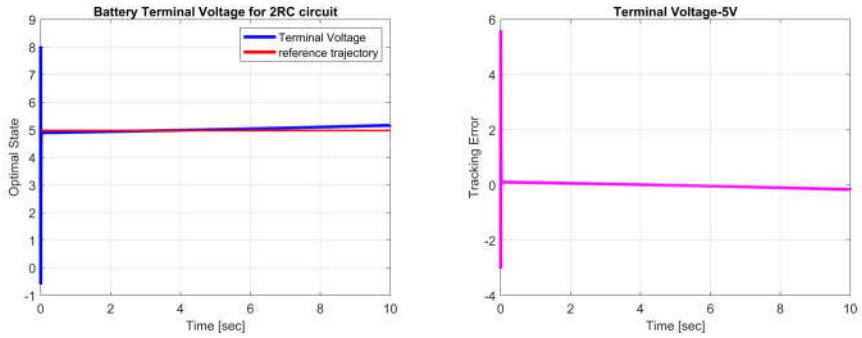

(a) (b)

Figure 2: a Desired and Actual Trajectories for 5V tracking. b Error in 5V tracking

b. Results for 12 Volts Tracking

A constant 12-volts curve was considered as a reference voltage. After the ephemeral overshoot the terminal voltage curve nearly caught up with the reference voltage. Figure 3 shows the simulation of first three seconds. During this period, the difference between the trajectories is little larger. However, in the last 7 seconds of the simulation, the terminal voltage caught up with the reference voltage and showed a good tracking performance. The charging scenario and the associated error are shown in Figure 4(a) and Figure 4(b) respectively.

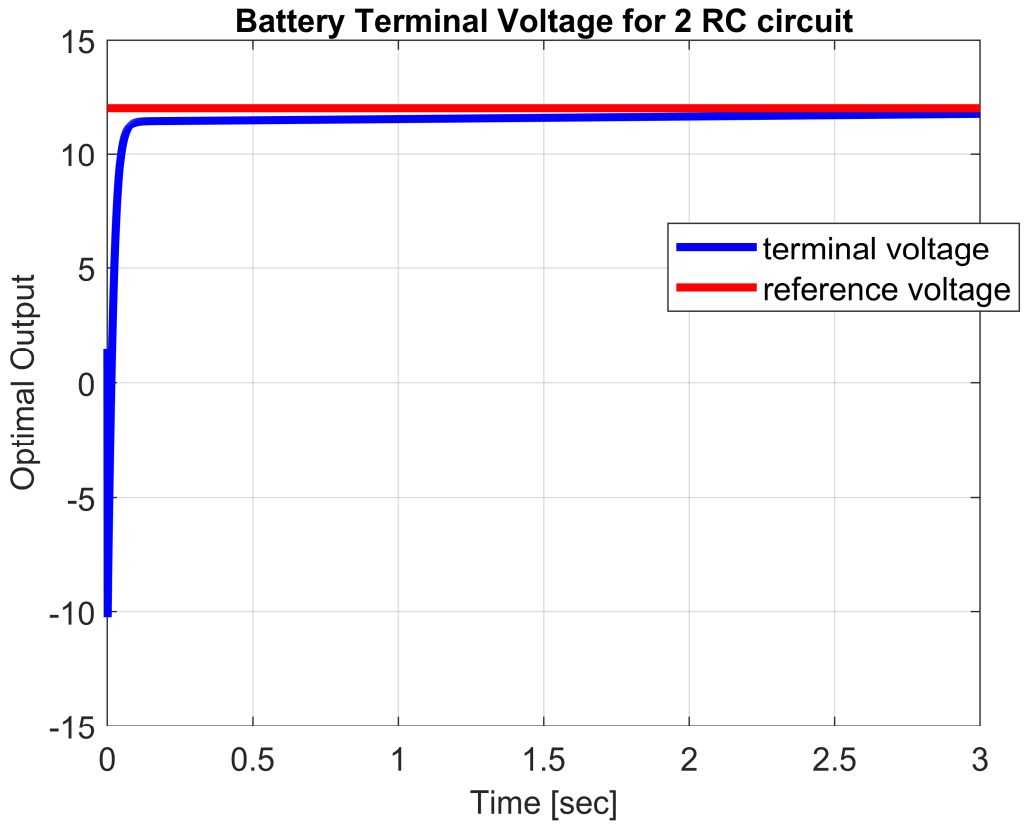

Figure 3: Initial difference between trajectories

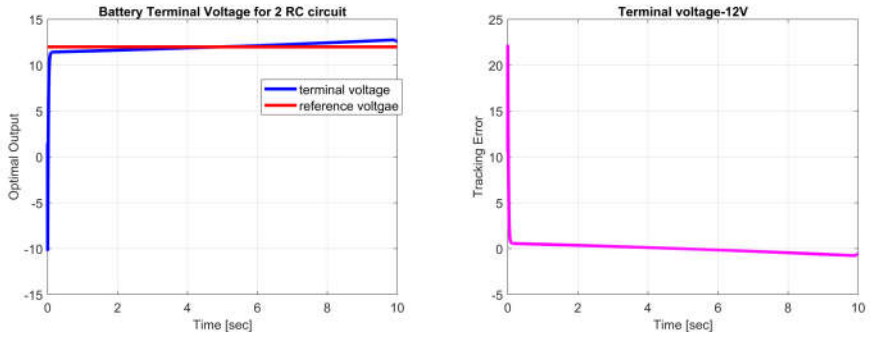

(a) (b)

Figure 4: a Desired and Actual Trajectories for 12V tracking. b Error in 12V tracking

V Conclusion

This paper provides an advanced tracking strategy for a nonlinear 2-RC EV battery model. With the use of SDRE technique for a finite horizon tracking system, a closed-loop optimal controller was obtained. The optimal controller minimized the quadratic error between the reference and actual trajectories. The MATLAB simulation shows that this optimal controller is indeed a very robust one in tracking reference trajectories of 5V and 12V. In future, a multiple-time-constant 3-RC EECM of an EV battery will be used to determine a new tracking strategy.

Bibliography

[1] Ryan Ahmed, Javier Gazzarri, Simona Onori, Saeid Habibi, Robyn Jackey, Kevin Rzemien, Jimi Tjong, and Jonathan LeSage. Model-based parameter identification of healthy and aged li-ion batteries for electric vehicle applications. *SAE International Journal of Alternative Powertrains*, 4(2):233–247, 2015.

[2] M Barnola-Sampera, D Heredero-Peris, R Villafafila-Robles, D Montesinos-Miracle, J Bergas-Jane, and N Vidal-Tejedor. Charging/discharging process for electric vehicles: Proposal and emulation. In *2014 IEEE International Electric Vehicle Conference (IEVC)*, pages 1–8. IEEE, 2014.

[3] A Barraud. A new numerical solution of = a_ {1} x+ xa_ {2}+ d, x (0)= c. *IEEE Transactions on Automatic Control*, 22(6):976–977, 1977.

[4] Yue Cao, Ryan C Kroeze, and Philip T Krein. Multi-timescale parametric electrical battery model for use in dynamic electric vehicle simulations. *IEEE Transactions on Transportation Electrification*, 2(4):432–442, 2016.

[5] T. Çimen. Development and validation of a mathematical model for control of constrained nonlinear oil tanker motion. *Mathematical and Computer Modeling of Dynamical Systems*, 15(1):1749, 2009.

[6] Cheng-Hung Chen. *Hybrid control strategies for smart prosthetic hand*. Idaho State University, 2009.

[7] F Claude, M Becherif, and HS Ramadan. Experimental validation for li-ion battery modeling using extended kalman filters. *International Journal of Hydrogen Energy*, 42(40):25509–25517, 2017.

[8] J.R. Cloutier. State-dependent Riccati equation techniques: An overview. *Proc. American Control Conference*, 2:932–936, 1997.

[9] Ozan Erdinc, Bulent Vural, and Mehmet Uzunoglu. A dynamic lithium-ion battery model considering the effects of temperature and capacity fading. In *2009 International Conference on Clean Electrical Power*, pages 383–386. IEEE, 2009.

[10] Zoran Gajic and Muhammad Tahir Javed Qureshi. *Lyapunov matrix equation in system stability and control*. Courier Corporation, 2008.

[11] Zhai Haizhou. Modeling of lithium-ion battery for charging/discharging characteristics based on circuit model. *International Journal of Online Engineering*, 13(6), 2017.

[12] Krishnan S Hariharan and V Senthil Kumar. A nonlinear equivalent circuit model for lithium ion cells. *Journal of power sources*, 222:210–217, 2013.

[13] Tarun Huria, Massimo Ceraolo, Javier Gazzarri, and Robyn Jackey. High fidelity electrical model with thermal dependence for characterization and simulation of high power lithium battery cells. In *2012 IEEE International Electric Vehicle Conference*, pages 1–8. IEEE, 2012.

[14] Tarun Huria, Massimo Ceraolo, Javier Gazzarri, and Robyn Jackey. Simplified extended kalman filter observer for soc estimation of commercial power-oriented lfp lithium battery cells. Technical report, SAE Technical Paper, 2013.

[15] Ibrahim Baz Khallouf and Desineni Subbaram Naidu. Advanced control strategies for the robotic hand. In *2018 IEEE 14th International Conference on Control and Automation (ICCA)*, pages 698–703. IEEE, 2018.

[16] AHMED Khamis and D Naidu. Nonlinear optimal tracking using finite horizon state dependent riccati equation (sdre). In *Proceedings of the 4th International Conference on Circuits, Systems, Control, Signals (WSEAS)*, pages 37–42, 2013.

[17] Ahmed Khamis, Hoa M Nguyen, and D Subbaram Naidu. Nonlinear optimal control of wind energy conversion systems with incomplete state information using sd-dre. In *2016 International Conference on Control, Decision and Information Technologies (CoDIT)*, pages 059–064. IEEE, 2016.

[18] Farid Khoucha, MEH Benbouzid, and Abdelaziz Kheloui. An optimal fuzzy logic power sharing strategy for parallel hybrid electric vehicles. In *2010 IEEE Vehicle Power and Propulsion Conference*, pages 1–5. IEEE, 2010.

[19] Ryan C Kroeze and Philip T Krein. Electrical battery model for use in dynamic electric vehicle simulations. In *2008 IEEE Power Electronics Specialists Conference*, pages 1336–1342. IEEE, 2008.

[20] Juuso Lindgren, Imran Asghar, and Peter D Lund. A hybrid lithium-ion battery model for system-level analyses. *International Journal of Energy Research*, 40(11):1576–1592, 2016.

[21] Jinkun Liu. *Intelligent Control Design and MATLAB Simulation*. Springer, 2018.

[22] H Miniguano, C Raga, A Barrado, A Lázaro, P Zumel, and E Olías. A comparative study and parameterization of electrical battery models applied to hybrid electric vehicles. In *2016 International Conference on Electrical Systems for Aircraft, Railway, Ship Propulsion and Road Vehicles & International Transportation Electrification Conference (ESARS-ITEC)*, pages 1–6. IEEE, 2016.

[23] D Subbaram Naidu. *Optimal control systems*. CRC press, 2002.

[24] D Subbaram Naidu, Sudipta Paul, and Craig R Rieger. A simplified SDRE technique for regulation in optimal control systems. In *2019 IEEE International Conference on Electro Information Technology (EIT)*. IEEE, in press.

[25] Anand Narayan. State and parametric estimation of li-ion batteries in electrified vehicles, 2017.

[26] J. Nazarzadeh, M. Razzaghi, and K. Nikravesh. Solution of the matrix Riccati equation for the linear quadratic control problems. *Mathematical and Computer Modelling*, 27(7):51–55, 1998.

[27] T. Nguyen and Z. Gajic. Solving the matrix differential Riccati equation: a Lyapunov equation approach. *IEEE Trans. Automatic Control*, 55(1):191–194, 2010.

[28] Gregory L Plett. Extended kalman filtering for battery management systems of lipb-based hev battery packs: Part 3. state and parameter estimation. *Journal of Power sources*, 134(2):277–292, 2004.

[29] Miguel Rodríguez Asensio. Modelling and state estimation of batteries. 2016.

[30] Zhe Ci Tang, Chun Lin Guo, and Dong Ming Jia. Analysis of electric vehicle battery charging and discharging. In *Applied Mechanics and Materials*, volume 556, pages 1879–1883. Trans Tech Publ, 2014.

[31] Olivier Tremblay, Louis-A Dessaint, and Abdel-Illah Dekkiche. A generic battery model for the dynamic simulation of hybrid electric vehicles. In *2007 IEEE Vehicle Power and Propulsion Conference*, pages 284–289. Ieee, 2007.

[32] L. Vandenberghe, V. Balakrishnan, R. Wallin, A. Hansson, and T. Roh. *Positive Polynomials in Control*, volume 312, chapter Interior-point methods for semidefinite programming problems derived from the KYP lemma, pages 195–238. D. Henrion and A. Garulli, Eds. Berlin, Germany: Springer Verlag, 2005.

[33] S Wijewardana, R Vepa, and MH Shaheed. Dynamic battery cell model and state of charge estimation. *Journal of Power Sources*, 308:109–120, 2016.

[34] Lotfi A Zadeh. Fuzzy sets, information and control. *vol*, 8:338–353, 1965.